

$^{15}\text{N}$  Nuclear Magnetic Resonance Studies of  
the Liver Alcohol Dehydrogenase- $\text{NAD}^+$ -Pyrazole Complex

Thesis by  
Nancy Newton Becker

In Partial Fulfillment of the Requirements  
for the Degree of  
Doctor of Philosophy

California Institute of Technology  
Pasadena, California

1983

(Submitted April 12, 1983)

To Michael, Daniel, and #2.



### Acknowledgments

I would like to thank my thesis advisor, Professor John D. Roberts, for his help throughout my years as a graduate student. I feel fortunate to have had his guidance during the course of this study. I would also like to thank the previous members of his research group. I am especially grateful to Dr. Keiko Kanamori, whose help has been invaluable.

I also would like to thank Professor John H. Richards and the members of his research group, for making available their research equipment.

I am grateful to Mrs. Rose Meldrum for her illustrations and help.

## ABSTRACT

<sup>15</sup>N Nuclear Magnetic Resonance Studies of the  
Liver Alcohol Dehydrogenase-NAD<sup>+</sup>-Pyrazole Complex

The structures of the liver alcohol dehydrogenase (LADH)-NAD<sup>+</sup>-pyrazole and LADH-NAD<sup>+</sup>-4-ethylpyrazole complexes were investigated by <sup>15</sup>N nuclear magnetic resonance (NMR) spectroscopy. <sup>15</sup>N chemical shifts were obtained for <sup>15</sup>N-labeled inhibitors and <sup>15</sup>N-labeled coenzyme bound in the enzyme ternary complexes. The structures of the two inhibitor complexes were found to be very similar. <sup>15</sup>N chemical shifts of various pyrazole derivatives were determined. <sup>15</sup>N NMR studies of model pyrazole derivative-zinc chloride complexes were carried out to determine the effect of zinc complexation on the pyrazole N2 chemical shift. The N1 nicotinamide resonance of the coenzyme of the LADH-NAD<sup>+</sup>-pyrazole complex was 96 ppm upfield from that of NAD<sup>+</sup> in solution and only 13 ppm downfield from that of NADH in solution, demonstrating formation of a derivative of dihydronicotinamide. The <sup>15</sup>N chemical shift of the pyrazole N1 of the ternary complex when compared to other pyrazole derivatives indicated bond formation between pyrazole N1 and the nicotinamide ring of the coenzyme. The <sup>15</sup>N shift of the

pyrazole N1 of the model pyrazole-NAD<sup>+</sup> adduct, N-benzyl-1,4-dihydro-4-pyrazolynicotinamide, was 5.8 ppm downfield from that of N1 of the enzyme ternary complex. The <sup>15</sup>N chemical shift of the pyrazole N2 of the ternary complex compared to pyrazole derivatives in solution was shielded by more than 40 ppm, demonstrating direct complexation of N2 to the active-site zinc. The results of model zinc complex studies indicated 60-100% inner-sphere coordination of the pyrazole N2 to the active-site zinc in the ternary complex.

## TABLE OF CONTENTS

	Page
Introduction	
I. Liver Alcohol Dehydrogenase.....	1
II. Pyrazole.....	6
III. Nuclear Magnetic Resonance.....	10
IV. NMR of LADH.....	13
Experimental.....	19
Results.....	23
Discussion	
I. Introduction.....	42
II. Coenzyme.....	42
III. Pyrazole	
1. Introduction.....	50
2. $^{15}\text{N}$ NMR of Pyrazole.....	52
3. $^{15}\text{N}$ Chemical Shifts of Model	
N-Substituted Pyrazoles.....	55
4. $^{15}\text{N}$ Chemical Shifts of Model	
Pyrazole-Zinc Complexes .....	60
5. $^{15}\text{N}$ Chemical Shifts of the	
Enzyme Ternary Complexes.....	72
IV. $^{15}\text{N}$ NMR Linewidths.....	79
V. Relevance to Mechanism of LADH.....	88
Conclusions.....	91
References.....	92

## LIST OF TABLES

Table	Title	Page
1	$^{15}\text{N}$ Chemical Shifts of the Enzyme Ternary Complexes and the Model Pyrazole- $\text{NAD}^+$ Adduct .....	24
2	$^{15}\text{N}$ Chemical Shifts of Pyrazole and Pyrazole Derivatives.....	30
3	Ultraviolet Absorption Maxima of Dihydronicotinamide Derivatives.....	34
4	$^{15}\text{N}$ Chemical Shifts of Reaction Products of Pyrazole and $\text{N}$ -Benzylnicotinamidinium Chloride VI or $\text{N}$ -Benzylnikethamidinium Chloride.....	36
5	$^{15}\text{N}$ Chemical Shifts of Zinc Complexes of Pyrazole and Pyrazole Derivatives.....	38
6	Effects of Zinc Complexation on $^{15}\text{N}$ Chemical Shifts of 2 Methyl-2-Pyrazolylethanoate.....	39
7	$^{13}\text{C}$ NMR Chemical Shifts of the Model Pyrazole- $\text{NAD}^+$ Adduct V and $\text{N}$ -Benzyl-1,4-dihydronicotinamide VII .....	46
8	$^{15}\text{N}$ Linewidths of the Enzyme Ternary Complexes.....	80

## LIST OF FIGURES

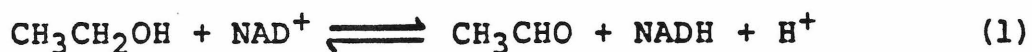
Figure	Title	Page
1	Dimeric LADH with Bound Coenzyme.....	2
2	Active Site of LADH.....	2
3	Proposed Formation and Structure of the LADH- NAD <sup>+</sup> -Pyrazole Complex .....	8
4	<sup>15</sup> N Spectra at 18.25 MHz of LADH-NAD <sup>+</sup> -Pyrazole Prepared from <sup>15</sup> N-Labeled Pyrazole.....	25
5	<sup>15</sup> N Spectra at 50.68 MHz of LADH-NAD <sup>+</sup> -Pyrazole Prepared from <sup>15</sup> N-Labeled Pyrazole and NAD <sup>+</sup> .....	26
6	<sup>15</sup> N Spectrum at 50.68 MHz of LADH-NAD <sup>+</sup> - 4-Ethylpyrazole Prepared from <sup>15</sup> N-Labeled 4-Ethylpyrazole.....	27
7	Other Possible Products of Pyrazole Addition to NAD <sup>+</sup> .....	44
8	Resonance Forms of NADH.....	48
9	Acid-Base Behavior of Pyrazole.....	51
10	Formation of the Model Pyrazole-NAD <sup>+</sup> Adduct.....	57
11	Proposed Sites of Zinc Complexation of Several Nucleosides.....	62
12	Proposed Sites of Zinc Complexation of Ethyl 2-Pyrazolyethanoate(IV).....	67

13	Proposed Structure of the N-Methylpyrazole-Zinc Chloride Complex IX $(\text{N-Methylpyrazole})_2\text{ZnCl}_2$ .....	67
14	Plot of Linewidth, $\nu_{1/2}$ , <u>versus</u> Effective Correlation Time, $\tau_{\text{eff}}$ , Assuming Dipolar Relaxation.....	81
15	Proposed Structure of LADH-NAD <sup>+</sup> -Pyrazole.....	89
16	Proposed Structure of the Transition State of the LADH Oxidation of Alcohol.....	89

## INTRODUCTION

I. Liver Alcohol Dehydrogenase

Liver alcohol dehydrogenase (LADH) is a zinc-containing enzyme of MW about 80,000 which catalyzes the reversible oxidation of ethanol to ethanal in the liver.<sup>1,2</sup> The reaction (Equation 1) is  $\text{NAD}^+$ -dependent, with equilibrium lying in favor of ethanol formation.



The reaction may be followed spectrophotometrically by observing the increase in absorbance at 340 nm arising from formation of NADH.

The amino-acid sequence of LADH has been determined.<sup>3</sup> The enzyme from horse liver, which is the subject of this thesis, is highly homologous (about 90%) to that from human liver<sup>4</sup> and less so to that from yeast.<sup>5</sup> The crystal structure of uncomplexed LADH has been determined to 2.4 Å resolution<sup>6</sup> and the crystal structures of several substrate or inhibitor ternary complexes with coenzyme have also been determined.<sup>7-11</sup>

LADH is a dimer, each identical subunit being of MW 40,000, and containing two zincs. One zinc is structural, liganded to four cysteine residues, Cys-97, Cys-100, Cys-



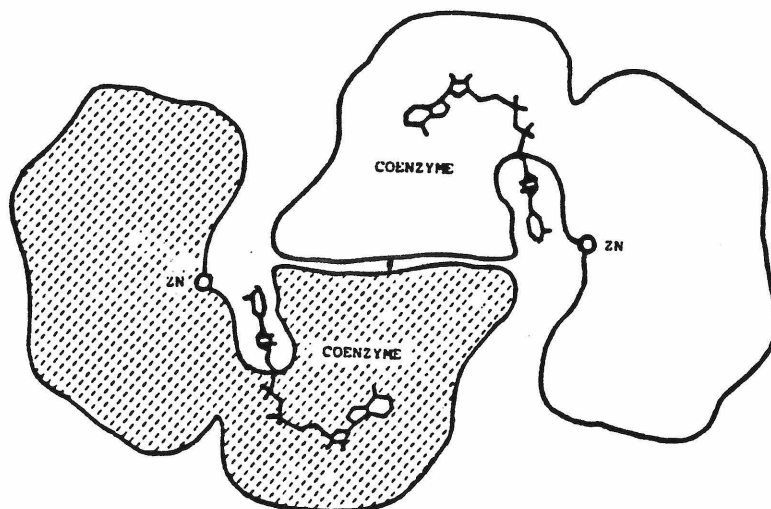


Figure 1. Dimeric LADH with Bound Coenzyme (from reference 12).

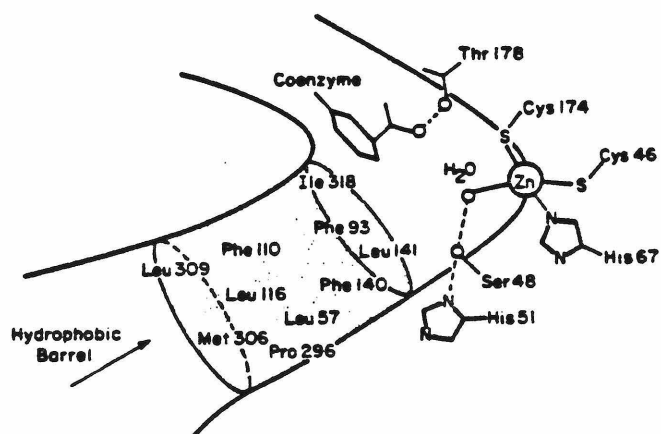


Figure 2. Active Site of LADH (from reference 2).

103, and Cys-111, in a distorted tetrahedral array. The other zinc is at the active site, liganded to two cysteines, Cys-46 and Cys-174, and one histidine, His-67, and one water molecule or hydroxide ion, again in a distorted tetrahedral arrangement.

The dimers form a dumbbell-shaped molecule, each monomer unit contributing residues to each active-site region as illustrated in Figure 1.<sup>12</sup> The active site has a non-specific substrate-binding region, capable of binding a variety of substrates and inhibitors in close proximity to both the catalytic zinc and the nicotinamide ring of bound coenzyme as in Figure 2.<sup>2</sup> This substrate-binding region has a hydrophobic, barrel-shaped pocket extending away from the active-site zinc, which strongly binds substrates or inhibitors with long, straight alkyl chains that can extend into this hydrophobic barrel.

The coenzyme-binding region consists of residues which bind adenosine diphosphate ribose (ADPR) in a manner similar to the ADPR moiety of  $\text{NAD}^+$  and NADH.  $\text{NAD}^+$  is bound more loosely than ADPR, indicating repulsion between the positively charged nicotinamide ring and active-site entities, probably including the active-site zinc. There is a conformational change upon  $\text{NAD}^+$  or NADH binding, resulting in reduced access of solvent to the active site. Binding of

a substrate reduces access further, resulting in a hydrophobic environment at the active site. The amide group is required for correct coenzyme binding and the subsequent conformational change, the pyridine ring extending away from the substrate-binding region, into solution, in its absence.<sup>13</sup>

Horse LADH is found to consist of a mixture of isozymes. There are mainly two types of monomer, each with different substrate specificity, the ethanol-specific monomer (designated "E"), and the steroid-specific monomer (designated "S"). The monomers themselves are not active, but combine to form three active isozymes, EE, SS, and ES. We are concerned here only with the EE isozyme, this being commercially available in 90% purity (based on isozyme content) as the crystalline suspension.

The catalytic mechanism of LADH has been reviewed recently by Klinman.<sup>2</sup> The major kinetic pathway (Figure 3) involves a compulsory-ordered mechanism,<sup>14</sup> with initial binding of coenzyme leading to a conformational change, and subsequent binding of substrate. Binding of  $\text{NAD}^+$  perturbs the  $\text{pK}_a$  of a group on the enzyme from 9.2 to 7.6,<sup>15</sup> this group possibly being zinc-bound water. Other zinc enzymes, such as carbonic anhydrase,<sup>16</sup> and zinc complex models in water solution<sup>17</sup> have demonstrated a large  $\text{pK}_a$  change of

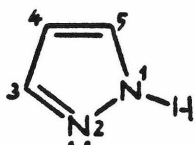
water upon binding to ligand-coordinated zinc. Binding of imidazole, demonstrated by X-ray crystallography<sup>18</sup> to displace zinc-bound water, removes the pH-dependence of NAD<sup>+</sup> binding. Direct hydride transfer has been demonstrated,<sup>2</sup> although there is still debate about the precise mechanism. Substrate binding may involve direct coordination to the active-site zinc, as indicated by the X-ray results for p-bromobenzyl alcohol binding.<sup>7</sup> This coordination implicates the active-site zinc as a Lewis acid in catalysis. High-field paramagnetic relaxation studies<sup>19-22</sup> of enzyme substituted with cobalt for zinc have been interpreted as demonstrating outer-sphere coordination of substrate or inhibitor to the active-site metal, suggesting that metal-bound water or hydroxide ion acts as a general acid-base catalyst in the LADH reaction.

The structure of inhibitor complexes may give insight to the role of the active-site zinc in substrate binding and in catalysis. The X-ray crystal structure of the LADH-NADH-dimethyl sulfoxide inhibitor complex at 2.9 Å resolution demonstrates direct coordination of inhibitor to zinc, the water being displaced as the fourth ligand.<sup>8</sup> The crystal structures of LADH complexes of imidazole and of 1,10-phenanthroline,<sup>18</sup> each of which is an inhibitor with metal-coordinating nitrogens, have demonstrated direct

coordination of inhibitor to the active-site zinc. More recently, the crystal structure of the LADH-NAD<sup>+</sup>-pyrazole complex has been published by Eklund and coworkers to 2.9 Å resolution.<sup>9</sup> The results again indicate direct coordination of pyrazole to zinc.

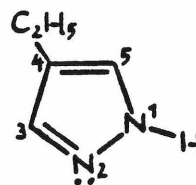
## II. Pyrazole

The structure of the LADH-NAD<sup>+</sup>-pyrazole complex is important as a possible model for the transition-state of LADH-mediated NAD<sup>+</sup> oxidation of alcohols. Pyrazole as an *in vivo* inhibitor of LADH is also important medically. Thus, pyrazole and its 4-substituted derivatives have been investigated for use in possible treatments of alcoholism and of methanol and ethylene glycol poisoning.<sup>23</sup>



Pyrazole

I



4-Ethylpyrazole

II

Pyrazole (I) was found to be a potent ethanol-competitive inhibitor of LADH by Theorell and Yonetani in

1963.<sup>24</sup> In the presence of  $\text{NAD}^+$ , it forms a tight ternary enzyme complex with a  $K_I$  of  $0.2 \mu\text{M}$ <sup>25</sup> and a lifetime of 25 sec at pH 7.<sup>26</sup> A less toxic derivative of pyrazole, 4-ethylpyrazole (II), is an even stronger inhibitor of LADH, with a  $K_I$  of  $0.007 \mu\text{M}$  in the presence of  $\text{NAD}^+$ .<sup>27</sup>

LADH- $\text{NAD}^+$ -pyrazole complex formation is accompanied by the liberation of 0.8 of a proton equivalent. The complex crystallizes in triclinic form, similar to the LADH-NADH-dimethyl sulfoxide complex and the binary LADH-coenzyme complex, while the apoenzyme crystallizes in orthorhombic form. The ultraviolet spectrum shows that formation of the LADH- $\text{NAD}^+$ -pyrazole complex is accompanied by an absorption increase at 290 nm, while pyrazole alone does not affect the LADH spectrum. This behavior is similar to that reported for the LADH- $\text{NAD}^+$ - $\text{NH}_2\text{OH}$  complex and other 1,4-dihydronicotinamide derivatives,<sup>24,28</sup> suggesting that the spectral change is caused by dihydronicotinamide formation in the enzyme ternary complex.

On the basis of evidence such as the above, Theorell

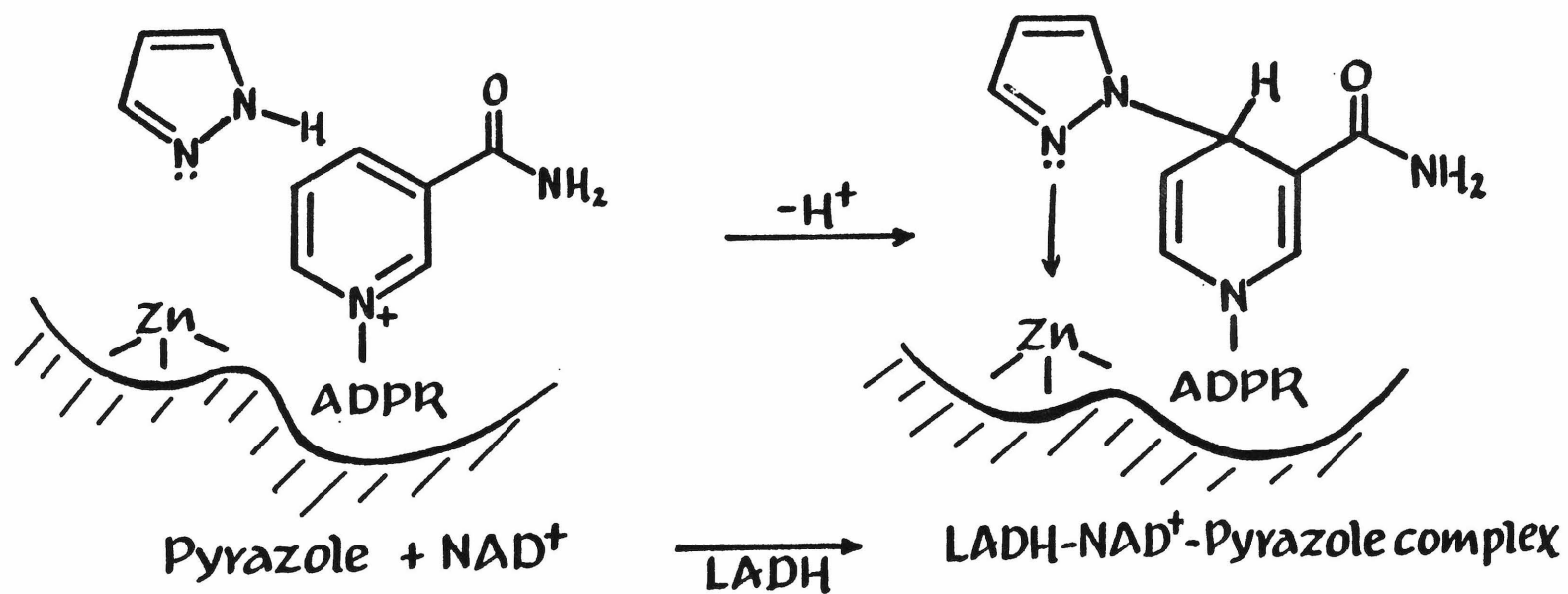


Figure 3. Proposed Formation and Structure of the LADH- $\text{NAD}^+$ -Pyrazole Complex.

and Yonetani proposed that N1 of pyrazole forms a covalent bond to C4 of the nicotinamide ring of the coenzyme in the ternary complex, with concurrent transfer of one equivalent of protons to solvent and/or enzyme residues. They also proposed on the basis of the zinc-complexing ability of pyrazole in solution, that N2 of the pyrazole derivative is directly coordinated to the active-site zinc atom. The proposed structure is shown in Figure 3.

Crystal structures of various LADH complexes without pyrazole which demonstrate that the nicotinamide ring is held in an orientation where the C6 side of the ring is directed toward the substrate-binding pocket and active-site zinc support the proposition that addition of pyrazole to the nicotinamide ring of the coenzyme should not occur at C2, but do also allow that addition could conceivably occur at C6 as well as at C4.<sup>7,8</sup> Angelis<sup>29</sup> has reported formation of a pyrazole-N-benzylnicotinamide adduct in solution with preferential addition at C4. It was not until recently, however, that proof of C4 addition in the enzyme complex was published. Eklund and coworkers<sup>9</sup> have found from X-ray studies at 2.9 Å resolution that in the crystalline LADH-NAD<sup>+</sup>-pyrazole complex, the pyrazole N1-nicotinamide C4 bond distance is 2 Å. This is about one-half angstrom longer than expected for a covalent bond of this type, and, if not



due to experimental error, could be due to the steric constraints at the active-site of the enzyme. The pyrazole N2-active-site zinc atom was determined to be 2.1 Å, indicative of inner-sphere coordination. However, Bobsein and Myers have interpreted  $^{113}\text{Cd}$  chemical shifts of the cadmium-substituted LADH-NAD<sup>+</sup>-pyrazole complex in solution as demonstrating outer-sphere coordination of the inhibitor to the active-site zinc.<sup>30</sup>

The possibility of inner-sphere coordination of inhibitor to the active-site metal in the crystalline complex, with outer-sphere coordination in solution has again been raised. Thus, it is important to study the structure of the native zinc-enzyme complexes in solution.

### III. Nuclear Magnetic Resonance

Nuclear magnetic resonance (NMR) is an important tool for the investigation of the structure and mechanism of enzymes. NMR of macromolecules presents problems usually not encountered in NMR of small molecules. Because the effective correlation time of a high-molecular-weight enzyme is long, both  $T_1$ , the longitudinal, and  $T_2$ , the transverse, relaxation times tend to be short. When  $T_2$  is short, the linewidths can become substantial as shown by the relation

$$\nu_{1/2} = \frac{1}{\pi T_2}$$

where  $\nu_{1/2}$  is the linewidth of the peak at half-height. This disadvantage is often offset by the opportunity for rapid pulsing allowed by short  $T_1$  relaxation times. While NMR of enzymes has more commonly involved the  $^1\text{H}$  and  $^{13}\text{C}$  nuclei,  $^{15}\text{N}$  NMR<sup>31</sup> for the study of enzymes has steadily increased.  $^{15}\text{N}$  has a nuclear spin of  $1/2$  and thus no quadrupole moment. Nitrogen is comparable in importance to oxygen biologically, and biochemical NMR studies of nitrogen nuclei have led to significant findings.<sup>32</sup>

The advantages of  $^{15}\text{N}$  NMR over  $^{13}\text{C}$  or  $^1\text{H}$  NMR include the greater range of chemical shifts, over 900 ppm, making resolution and assignment of resonances easier, and a nuclear Overhauser effect (NOE) of -3.9. While a full NOE will cause an approximately 4-fold signal enhancement upon proton decoupling, a partial NOE can decrease or even null a nitrogen resonance. In such circumstances, gated proton decoupling is helpful to remove  $^1\text{H}$ - $^{15}\text{N}$  coupling without generating NOE.

Other disadvantages include a low gyromagnetic ratio, leading to a sensitivity only  $1.04 \times 10^{-3}$  that of protons for equal numbers of nuclei and highly variable relaxation times. The sensitivity factor, combined with the low

natural abundance of  $^{15}\text{N}$  (0.37%), leads to a sensitivity at the natural-abundance level which is only  $3.8 \times 10^{-6}$  that of protons at similar molar concentrations of protons and nitrogens. The sensitivity problem can be greatly alleviated by the use of  $^{15}\text{N}$ -enriched compounds. Relaxation times of  $^{15}\text{N}$  nuclei vary greatly, from very much less than one second to several minutes<sup>31</sup> requiring adjustment of the pulse width and delay to allow observation of the slowest-relaxing nitrogens.

The taking of  $^{15}\text{N}$  NMR spectra of enzymes has until recently been restricted by the low concentrations obtainable for most large proteins. The advent of wide-bore spectrometers, which allows sample volumes of 18 ml or greater, has advanced the study of enzymes by  $^{15}\text{N}$  NMR at the natural-abundance level. In 1975, Gust, Moon, and Roberts<sup>33</sup> reported the natural-abundance  $^{15}\text{N}$  spectrum of lysozyme, an enzyme of MW 14,300.

The availability of  $^{15}\text{N}$ -enriched compounds has also contributed to the wider applicability of  $^{15}\text{N}$  NMR to enzyme systems. Bachovchin and Roberts<sup>34</sup> used  $^{15}\text{N}$  NMR of the selectively  $^{15}\text{N}$ -enriched histidine of  $\alpha$ -lytic protease to assist in elucidating the catalytic mechanism.  $^{15}\text{N}$ -enriched substrates and inhibitors have allowed studies of substrate and inhibitor complexes of enzymes by  $^{15}\text{N}$  NMR. These NMR

studies using  $^{15}\text{N}$ -enriched samples are still limited by the solubility of the enzyme, millimolar concentrations being required.

The greater sensitivity and resolution possible at higher magnetic fields has also aided the study of enzymes by NMR. However, higher magnetic fields may lead to appreciable line broadening in  $^{15}\text{N}$  NMR. This is because there may be a significant contribution to the transverse relaxation time  $T_2$  by chemical-shift anisotropy in  $^{15}\text{N}$  NMR, whereas in  $^{13}\text{C}$  NMR<sup>35</sup> and  $^1\text{H}$  NMR<sup>36</sup> dipolar relaxation usually dominates. The anisotropic portion of  $T_2$  is inversely proportional to the square of the field<sup>37</sup> and thus leads to a decrease in  $T_2$  and an increase in the linewidth as the field is increased.

#### IV. NMR of LADH

While no  $^{15}\text{N}$  NMR studies have previously been reported, LADH has been studied through the use of NMR of other nuclei, including  $^1\text{H}$ ,  $^{13}\text{C}$ ,  $^{19}\text{F}$  and  $^{113}\text{Cd}$ . Investigations of substrate- and coenzyme-LADH interactions have been made by determining the line-broadening of substrate or coenzyme upon exchange between bound and unbound states. Czeisler and Hollis<sup>38</sup> have used proton NMR of NADH in the presence of LADH to determine the lifetime of bound NADH. The proton

NMR studies of substrate binding by LADH reported by Hollis<sup>39</sup> indicate that the substrate is bound rigidly to LADH only in the presence of coenzyme.

Anderson and Dahlquist<sup>40</sup> have recently demonstrated through  $^{19}\text{F}$  NMR studies of trifluoroethanol (TFE) binding to LADH that biphasic kinetics are a property of a single site in LADH, where the other site has been inactivated by binding the pyrazole- $\text{NAD}^+$  complex. This result invalidates the proposal<sup>41</sup> that site-site interactions affect catalysis by LADH.

Anderson and Dahlquist<sup>42</sup> have also used fluorine NMR of trifluoroethanol binding to the LADH- $\text{NAD}^+$  complex to determine the bound lifetimes of TFE and pyrazole in the LADH- $\text{NAD}^+$ -TFE and LADH- $\text{NAD}^+$ -pyrazole complexes at pH 8.7 (40 sec and 400 sec, respectively). These investigators believe that the  $^{19}\text{F}$  shift of bound TFE in the LADH- $\text{NAD}^+$ -TFE complex does not favor TFE binding directly to the active-site zinc. The argument is that the  $^{19}\text{F}$  signal of the enzyme complex was shifted only slightly (0.28 ppm downfield), in the direction of the change in shift of TFE upon deprotonation (0.59 ppm downfield), whereas the fluorine resonances of the model adducts,  $(\text{TFE})(\text{ethyl})\text{Zn}$  and  $(\text{TFE})(\text{phenyl})\text{Zn}$  are shifted 1.7 and 3.4 ppm, respectively, upfield. However, the interpretation may be faulty, because the TFE may bind

as the alcoholate to the active-site zinc, with a partial cancellation of effects. The model zinc complexes may also be poor analogs of the zinc complex in the enzyme. Also, possible effects of enzyme residues must be considered. The authors do state that their results are consistent with the presence of a partial negative charge on the oxygen of bound TFE.

Nuclear magnetic relaxation studies have been performed using LADH with cobalt substituted for both the active-site and structural zincs. Mildvan and coworkers<sup>20,21</sup> have reported that relaxation rates of exchanging substrates and inhibitors indicate that these substances bind in the outer-coordination sphere of the paramagnetic cobalt in LADH complexes. While their work has been criticized because the degree of cobalt substitution of the active-site zinc was questionable, Drysdale and Hollis<sup>22</sup> used a well-characterized, fully cobalt-substituted LADH to study the binding of substrates and inhibitors. Their results were in agreement with those of Mildvan and coworkers,<sup>43</sup> indicating outer-sphere coordination of dimethyl sulfoxide and TFE to the LADH-NAD<sup>+</sup>-inhibitor complexes.

These results conflict with those of X-ray crystallographic studies of LADH complexes, which indicate direct binding of *p*-bromobenzyl alcohol<sup>7</sup> and dimethyl

sulfoxide<sup>8</sup> to the active-site zinc of the LADH-NAD<sup>+</sup>-substrate and LADH-NADH-inhibitor complexes, respectively. This has led to the suggestion that the crystal structures may not represent the active enzyme in solution. However, Andersson *et al.*<sup>44</sup> have reinvestigated the cobalt-substituted enzyme at various field strengths. They could detect no paramagnetic contribution from the Co<sup>II</sup> ions to the relaxation rate of solvent water and methanol protons, but they did find small variations in the diamagnetic contributions at different magnetic fields which might be mistaken for paramagnetic effects at the high fields used in the previous studies. Thus, paramagnetic effects were suggested to be small and reinterpretation of the earlier high-field experiments indicated.

Direct observation of the metal ion in the active site of cadmium-substituted LADH is possible by NMR because diamagnetic <sup>113</sup>Cd has a nuclear spin of 1/2. Bobsein and Myers<sup>30</sup> have reported that trifluorethanol and pyrazole in the ternary LADH-NAD<sup>+</sup>-inhibitor complexes of cadmium-substituted LADH must bind as outer-sphere complexes, on the basis of identical <sup>113</sup>Cd shifts for the two complexes. This interpretation has been criticized<sup>7</sup> because appropriate model compounds have not been prepared. Bobsein and Myers<sup>45</sup> did interpret the chemical shift of the LADH-imidazole

complex as being indicative of inner-sphere coordination to the metal, even though this chemical shift is only 1 ppm downfield from that of the pyrazole and trifluoroethanol complexes. The effect of pentacoordination must be considered, because  $\text{Cd}^{\text{II}}$  does not demonstrate as great a tendency for 4-coordinate over 5-coordinate complexes as does  $\text{Zn}^{\text{II}}$ .<sup>46</sup>

Furthermore, the complex designated by Bobsein and Myers<sup>30</sup> as the LADH- $\text{NAD}^+$  complex unexpectedly behaves like the LADH-NADH complex, with identical chemical shifts, proton-decoupling effects and pH-dependence, the pH-dependence being that expected for the LADH-NADH binary complex. Only a 2-fold excess of  $\text{NAD}^+$  was used to prepare the LADH- $\text{NAD}^+$  and trifluoroethanol complexes and only a 1-fold excess of  $\text{NAD}^+$  was used to prepare the LADH- $\text{NAD}^+$ -pyrazole complex (the order of addition of pyrazole and coenzyme not specified). Although the authors report the residual ethanol content to be no more than 20% of the active-site concentration, these results and procedures suggest that perhaps the coenzyme present in these complexes has been reduced to NADH. Because pyrazole and trifluoroethanol do not form very tight complexes with NADH, it is not surprising that they should lead to similar cadmium chemical shifts, in the absence of  $\text{NAD}^+$ , possibly



indicative of outer-sphere coordination.

Even if the complexes prepared were the appropriate ones, with oxidized coenzyme, and if the chemical shifts are actually indicative of outer-sphere coordination, this is not proof that inner-sphere coordination of pyrazole to zinc in the native LADH-NAD<sup>+</sup>-pyrazole complex does not occur. The catalytic activity of cadmium-substituted LADH is only 14% that of native LADH, which fact may indicate substantial alteration of the transition state for hydride transfer.<sup>46</sup> It is important to investigate the structure of complexes of the zinc-enzyme, as has been done in this thesis.

## EXPERIMENTAL

All reagents used were of reagent-grade purity unless otherwise specified.

$^{15}\text{N}_2$ -Pyrazole (99% isotopic abundance) was prepared from hydrazine sulfate- $^{15}\text{N}$  (Stohler, 99% isotopic abundance) and 1,1,3,3-tetraethoxypropane (Aldrich) by the method of Jones<sup>47</sup> and subsequently purified by sublimation.  $^{15}\text{N}_2$ -4-Ethylpyrazole was prepared in a similar manner using 1,1,3,3-tetraethoxy-2-ethylpropane prepared<sup>48</sup> from 1-ethoxy-1-butene.<sup>49</sup>  $[\text{N1-}^{15}\text{N}]\text{-NAD}^+$  was prepared from  $[\text{N1-}^{15}\text{N}]\text{-nicotinamide}$  (90% isotopic abundance) by the method of Oppenheimer and Davidson.<sup>50</sup>

The N-methylpyrazole-zinc chloride adduct was prepared by the addition of one molar equivalent of zinc chloride to a 1.3 M aqueous solution of N-methylpyrazole at pH 6. The resulting precipitate was dried, dissolved in chloroform and, after removal of solvent, the residue had a melting point of 102-108°. (Found: C, 31.56; H, 4.21; Cl, 24.23; N, 17.81; Zn, 22.35%.  $\text{C}_8\text{H}_{12}\text{N}_4\text{Cl}_2\text{Zn}$  requires: C, 31.99; H, 4.03; Cl, 23.60; N, 18.65; Zn, 21.74%.) Ethyl 2-pyrazolylethanoate was prepared from pyrazole and 2-bromoethyl ethanoate by the method of Jones.<sup>47</sup> N-Benzylpyrazole and N-allylpyrazole were prepared similarly from pyrazole and benzyl chloride or allyl bromide. N-

carbamoyl-3-methylpyrazole and 3,5-dimethylpyrazolylmethanol were purchased from Aldrich and used without further purification.

Zinc chloride (Ultrapure, >99% purity) was purchased from Alfa.

N-Benzylnicotinamidinium chloride was prepared according to the method of Karrer and Stare.<sup>51</sup> N-Benzylnikethamidinium chloride (N-benzyl-N,N-diethylnicotinamidinium chloride) was prepared in a similar manner from N,N-diethylnicotinamide (nikethamide, Sigma).

Pyrazole-substituted dihydronicotinamide derivatives were prepared by three different methods.

Method A The model pyrazole-nicotinamide adduct N-benzyl-1,4-dihydro-4-pyrazolylnicotinamide was prepared at room temperature by the addition of a 2.0 M solution of sodium hydroxide to an equimolar aqueous solution of pyrazole and N-benzylnicotinamidinium chloride, as described by Angelis.<sup>29</sup> The resultant yellow oil was extracted into chloroform and maintained at 0-8° to retard decomposition.

Method B An aqueous solution of 2.2 M pyrazole and 2.2 M sodium hydroxide was added to an equal volume of a 2 M aqueous solution of N-benzylnicotinamidinium chloride or N-benzylnikethamidinium chloride, layered with chloroform, at 0°. After removal of the chloroform layer, the aqueous

reaction mixture was further extracted with chloroform.

Method C An aqueous solution of pyrazole (40 mg, about 0.5 mM) and sodium hydroxide (1.1 equivalents) were added to an aqueous solution of excess (5-fold) N-benzylnicotinamidinium chloride, layered with chloroform at 0°.

LADH was purchased from Boehringer-Mannheim and dialyzed at 4° against 0.1 M phosphate buffer, pH 7.0, to remove residual ethanol. After addition first of pyrazole and subsequently of NAD<sup>+</sup> (10-fold and 15-fold excesses, respectively), the solutions were concentrated by ultracentrifugation at 4°. The LADH-NAD<sup>+</sup>-4-ethylpyrazole complex was prepared from undialyzed enzyme.

<sup>15</sup>N spectra of the ternary complex prepared from <sup>15</sup>N-labeled pyrazole and unlabeled NAD<sup>+</sup> were obtained on a Bruker WH-180 spectrometer operating at 18.25 MHz. Samples were contained in 25-mm tubes and were 1.1 mM (2.2 mM) in enzyme. The temperature for some samples was maintained at 12-14°. Others were at the ambient temperature. Inverse-gated, proton-decoupled spectra were obtained in about 24 hours using a 90°-pulse width and delay of 1.5-2 sec. <sup>15</sup>N spectra of the ternary complex prepared from both <sup>15</sup>N-labeled pyrazole and <sup>15</sup>N-labeled NAD<sup>+</sup> were obtained with a Bruker WM-500 spectrometer operating at 50.68 MHz. The

sample was contained in a 10-mm tube and was 1.5 mM (3 mM) in enzyme. The temperature was maintained at 4°. Inverse-gated, proton-decoupled spectra were obtained in about 12 hours using a 90°-pulse width and a 5-sec delay to avoid overheating.

The  $^{15}\text{N}$  spectrum of the ternary complex containing  $^{15}\text{N}$ -labeled 4-ethylpyrazole and unlabeled  $\text{NAD}^+$  was obtained with the Bruker WM-500 spectrometer at ambient temperature. The sample was contained in a 10-mm tube and was 1 mM (2 mM) in concentration. An inverse-gated, proton-decoupled spectrum was obtained in 24 hours using a 90° pulse width and a 2-sec delay.

$^{15}\text{N}$  spectra of the pyrazole derivatives were obtained with the Bruker WH-180, Bruker WM-500 or Varian XL-200 spectrometers using inverse-gated proton decoupling, a pulse width of 45°, and a delay of 15 sec. All  $^{15}\text{N}$  chemical shifts are reported in ppm upfield from external 1 M nitric acid in  $\text{D}_2\text{O}$  and are accurate to 0.1 ppm.

## RESULTS

Enzyme Complexes

The  $^{15}\text{N}$  chemical shifts of the LADH- $\text{NAD}^+$ -pyrazole and LADH- $\text{NAD}^+$ -4-ethylpyrazole complexes are collected in Table 1.

The  $^{15}\text{N}$  NMR spectra obtained at 18.25 MHz from the LADH- $\text{NAD}^+$ -pyrazole complex prepared from doubly- $^{15}\text{N}$ -labeled pyrazole are shown in Figure 4. The observed  $^{15}\text{N}$ - $^{15}\text{N}$  one-bond coupling constant,  $^1J_{\text{NN}}$ , for the two nonequivalent pyrazole nitrogens, N1 and N2, of the complex was  $10 \pm 2$  Hz. This coupling is similar to those reported for other  $\text{N}$ -substituted pyrazoles. Hawkes and coworkers<sup>52</sup> report a  $^1J_{\text{NN}}$  of 12.8 Hz for  $^{15}\text{N}$ -labeled  $\text{N}$ -phenylpyrazole, which is within the range reported by Bulusu and coworkers,<sup>53</sup> 4.5-19 Hz. The linewidths for proton-decoupled N1 and N2 doublets were approximately 16 and 20 Hz, respectively. The spectrum of dialyzed enzyme complex shown in Figure 4(b) demonstrates that the assigned resonances are indeed due to bound inhibitor which cannot be removed by dialysis.

The sample of the ternary complex prepared from both doubly  $^{15}\text{N}$ -labeled pyrazole and  $^{15}\text{N}$ -labeled  $\text{NAD}^+$  gave the 50.68 MHz spectra shown in Figure 5. The chemical shifts of the bound pyrazole nitrogens were identical to those found at 18.25 MHz, while the free pyrazole was different by +0.5

Table 1.  $^{15}\text{N}$  Chemical Shifts<sup>a</sup> of the Enzyme Ternary Complexes and the Model  
Pyrazole-NAD<sup>+</sup> Adduct

Solute	concn M	Solvent	$\delta^{15}\text{N}$		$\bar{\delta}^{15}\text{N}^b$	NADR
			Pyrazole N2	Pyrazole N1		
LADH-NAD <sup>+</sup> -pyrazole	$1.1 \times 10^{-3}$	Buffer <sup>c</sup>	117.8	142.1	129.95	247.2
LADH-NAD <sup>+</sup> -4-ethylpyrazole	$1 \times 10^{-3}$	Buffer <sup>c</sup>	119.0	146.0	132.5	---
Model Pyrazole-NAD <sup>+</sup> Adduct (N-benzyl-1,4-dihydro-4- pyrazolylnicotinamide, V)	~2	CHCl <sub>3</sub>	76.7	136.3	106.5	---

a In parts per million upfield from external 1 M nitric acid in D<sub>2</sub>O.

b Average shift of pyrazole nitrogens.

c 0.1 M sodium phosphate.

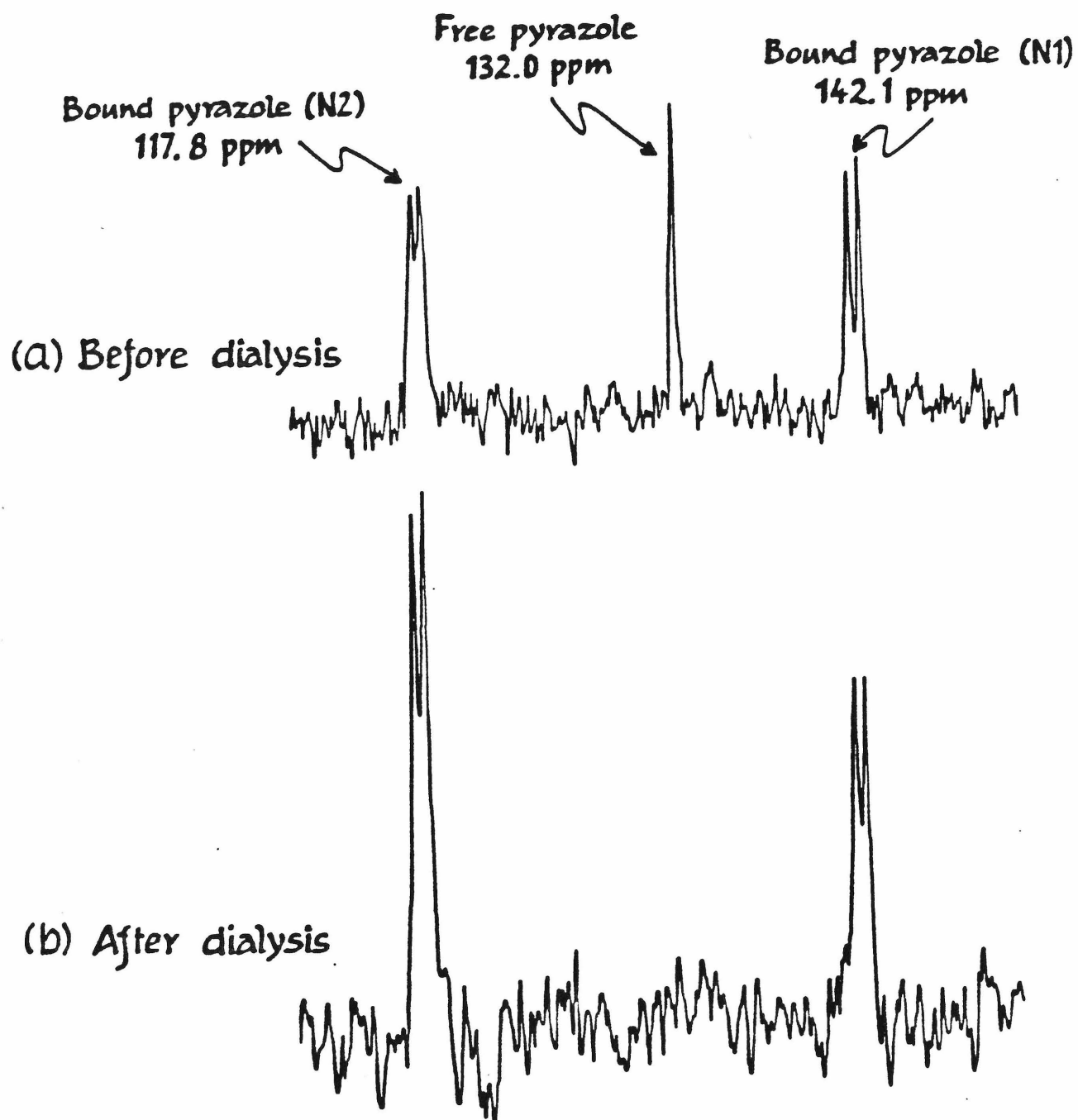


Figure 4.  $^{15}\text{N}$  Spectra at 18.25 MHz of LADH-NAD<sup>+</sup>-Pyrazole Prepared from  $^{15}\text{N}$ -Labeled Pyrazole.

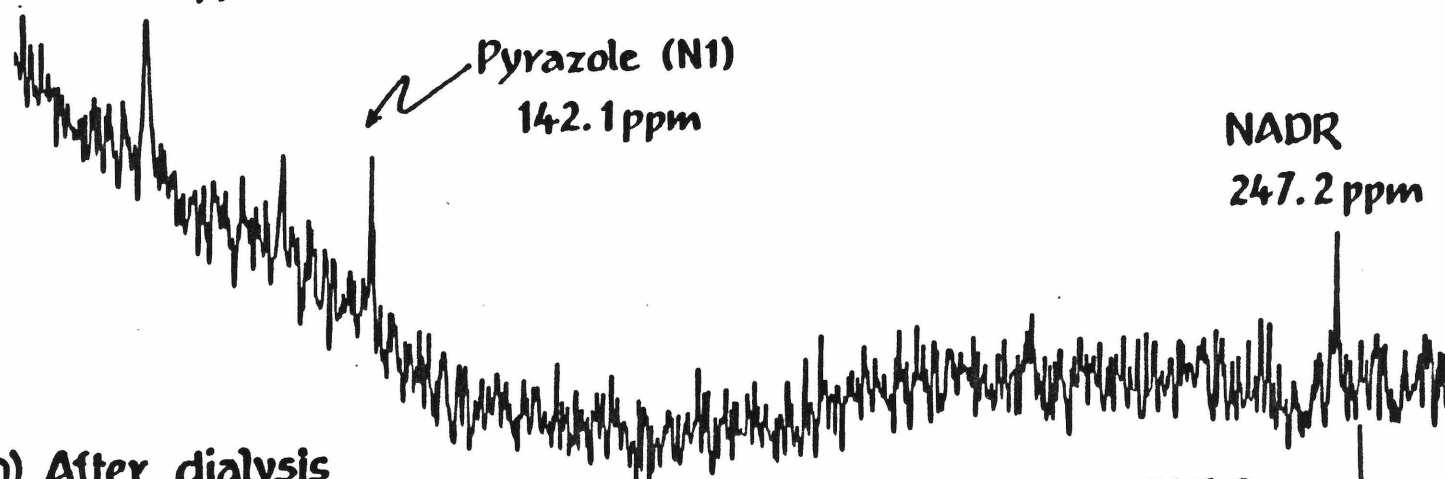
- (a) Before dialysis, proton-decoupled (21,783 transients).  
(b) After dialysis, proton-decoupled (27,007 transients).



(a) Before dialysis

Pyrazole (N2)

117.8 ppm



(b) After dialysis

117.8 ppm

142.1 ppm

247.2 ppm

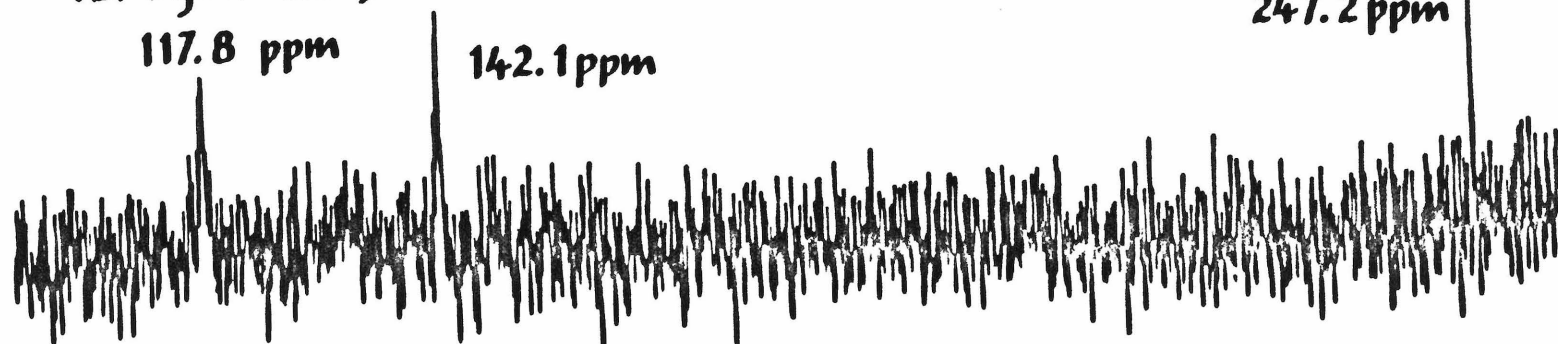


Figure 5. <sup>15</sup>N Spectra at 50.68 MHz of LADH-NAD<sup>+</sup>-Pyrazole Prepared from <sup>15</sup>N-Labeled Pyrazole and NAD<sup>+</sup>. (a) Before dialysis, proton-coupled, no delay between 90° pulses (43,000 transients) (b) After dialysis, proton-decoupled (5,725 transients).

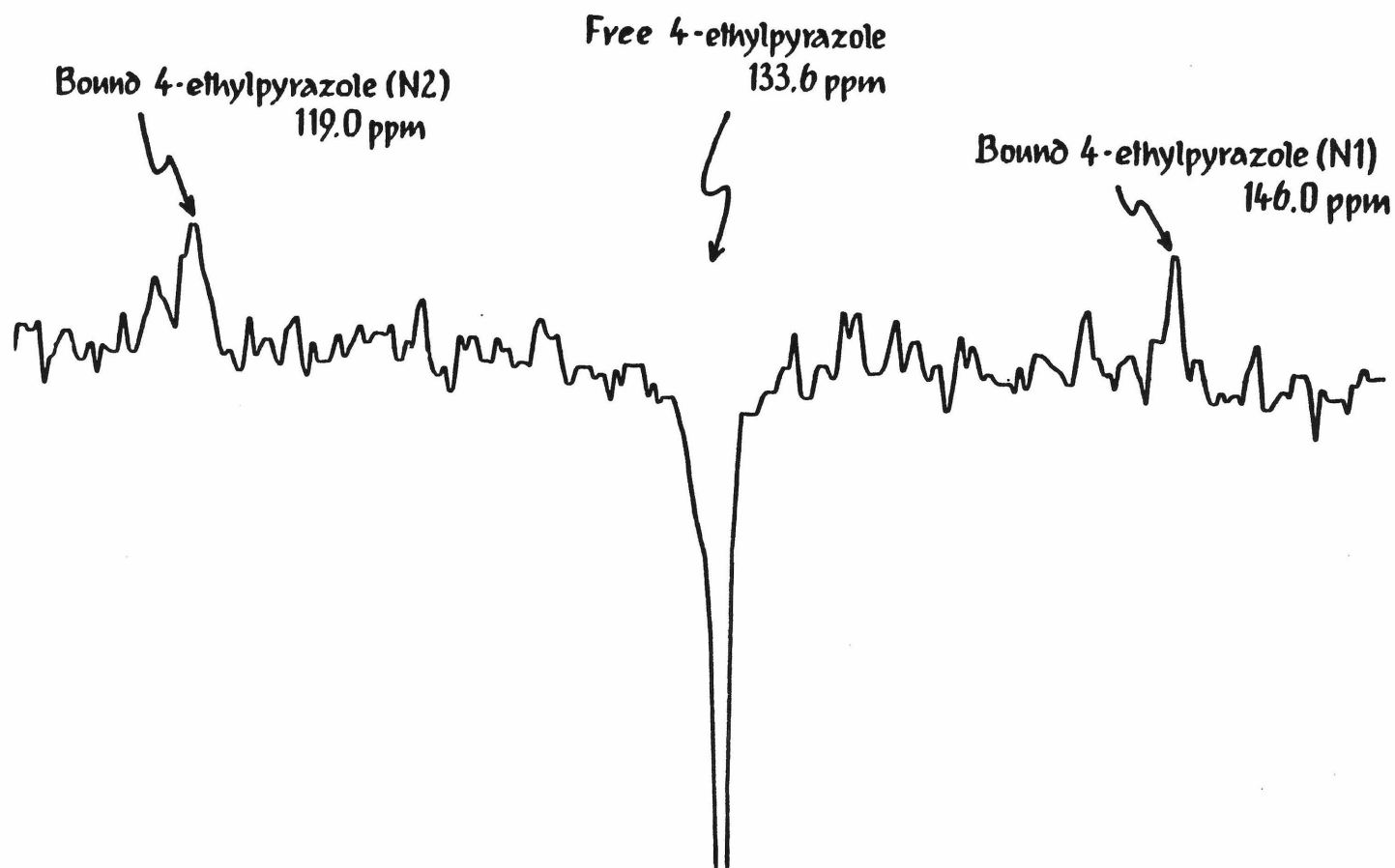


Figure 6.  $^{15}\text{N}$  Spectrum at 50.68 MHz of LADH-NAD $^{+}$ -4-Ethylpyrazole Prepared from  $^{15}\text{N}$ -Labeled 4-Ethylpyrazole. Undialyzed, proton-decoupled (74,356 transients), spectrum obtained by K. Kanamori.

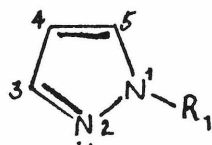
ppm. At the higher field, 50.68 ~~versus~~ 18.25 MHz, the  $^{15}\text{N}$ - $^{15}\text{N}$  coupling of the pyrazole nitrogens was unresolved, N1 and N2 each being broadened to about 25 and 30 Hz, respectively, in the proton-decoupled spectrum. This broadening is likely to be the consequence either of increases in relaxation rate associated with chemical-shift anisotropy or of chemical exchange. The chemical shift of the nicotinamide ring nitrogen (N1) of the coenzyme in the ternary complex is 96 ppm upfield from that of  $\text{NAD}^+$  in solution,<sup>50</sup> which fact indicates dihydronicotinamide formation, as will be discussed later. The observed linewidth for this nicotinamide nitrogen in the decoupled spectrum was about 5 Hz. Again, the spectrum obtained after dialysis (see Figure 5(b)) demonstrates that these resonances are due to bound inhibitor and coenzyme.

The sample of LADH- $\text{NAD}^+$ -4-ethylpyrazole complex prepared from doubly  $^{15}\text{N}$ -labeled 4-ethylpyrazole and unlabeled  $\text{NAD}^+$  gave the  $^{15}\text{N}$  spectrum at 50.68 MHz shown in Figure 6. The ternary complex was prepared from undialyzed enzyme which contained residual ethanol. This, however, should be irrelevant because 4-ethylpyrazole (added in large excess to the enzyme before the addition of excess  $\text{NAD}^+$ ) in the presence of  $\text{NAD}^+$  displaces ethanol completely. The chemical shifts for the bound pyrazole nitrogens, N1 and N2,

were 146.0 and 119.0 ppm, respectively, while the chemical shift for the unbound 4-ethylpyrazole was 133.6 ppm. The  $^{15}\text{N}$  one-bond coupling was unresolved because of line broadening, as in the earlier 50.68 MHz spectra. The linewidths for the N1 and N2 resonances were about 20 and 40 Hz, respectively. The operating conditions used to obtain the inverse-gated proton-decoupled spectrum for this complex were slightly different from those used for previous complexes, with a shorter delay time between pulses. This apparently led to an inverted free 4-ethylpyrazole resonance as the result of some residual NOE.

Also apparent in the spectra obtained from these ternary complexes is the broad resonance at about 255 ppm which can be assigned to the backbone amide nitrogens of the enzyme.

Table 2.  $^{15}\text{N}$  Chemical Shifts<sup>a</sup> of Pyrazole and Pyrazole Derivatives



solute	$\text{R}_1$	concn $\text{M}$	solvent	$\delta^{15}\text{N}$		$\bar{\delta}^{15}\text{N}^b$	Reference
				N2	N1		
Pyrazole (I)	-H	2	$\text{H}_2\text{O}$			132.8	54
		5	$\text{CH}_3\text{CN}$			125.5	this work
		1	$(\text{CH}_3)_2\text{SO}$	74.0	166.0	120.0	this work
$^{15}\text{N}_2$ -Pyrazole	-H	$6 \times 10^{-3}$	$\text{H}_2\text{O}$			132.1	this work
	-H	$10 \times 10^{-3}$	Buffer			132.0	this work
4-Ethylpyrazole (II)	-H	$10 \times 10^{-3}$	Buffer			133.6	this work
N-Methylpyrazole (III)	-H	2	$\text{CHCl}_3$	70.3	174.6	122.45	54
N-Benzylpyrazole	$-\text{CH}_2\text{C}_6\text{H}_5$		<u>neat</u>	68.9	162.8	115.85	this work
		2	$\text{CH}_3\text{CN}$	67.3	161.5	114.4	this work

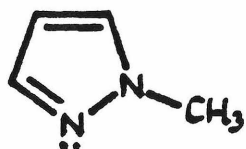
(continued)

Table 2, continued:

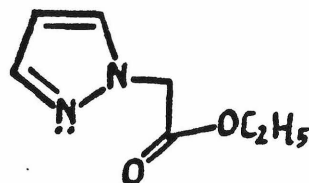
solute	R <sub>1</sub>	concn M	solvent	$\delta^{15}\text{N}$		$\bar{\delta}^{15}\text{N}^b$	Reference
				N2	N1		
Ethyl 2-pyrazolyl-ethanoate (IV)	-CH <sub>2</sub> COOC <sub>2</sub> H <sub>5</sub>	2	CH <sub>3</sub> CN	66.4	173.3	119.85	this work
		2	(CH <sub>3</sub> ) <sub>2</sub> SO	65.4	172.7	119.05	this work
N-Allylpyrazole	-CH <sub>2</sub> CH=CH <sub>2</sub>		neat	68.9	162.8	115.85	this work
		3	C <sub>2</sub> H <sub>5</sub> OH	76.7	167.3	122.0	this work
N-Carbamoyl-3-methylpyrazole	-CONH <sub>2</sub>	3	(CH <sub>3</sub> ) <sub>2</sub> SO	81.2	152.6	116.9	this work
3,5-Dimethylpyrazole	-H	2	CHCl <sub>3</sub>			133.6	54
3,5-Dimethyl-pyrazolylmethanol	-CH <sub>2</sub> OH	2	(CH <sub>3</sub> ) <sub>2</sub> SO	73.4	156.6	115.0	this work
N-Benzyl-1,4-dihydro-pyrazolyl-nicotinamide (V)		~2	CHCl <sub>3</sub>	76.7	136.3	106.5	this work

a In parts per million upfield from external 1 M nitric acid in D<sub>2</sub>O.

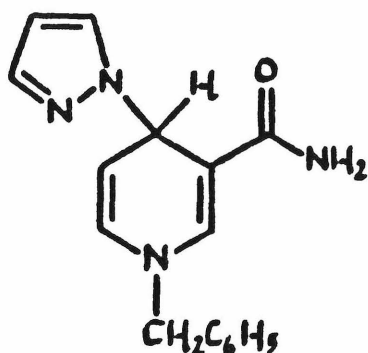
b Average shift of pyrazole nitrogens.

Pyrazole Derivatives

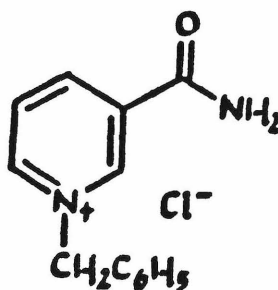
III



IV



V



VI

For comparison with the  $^{15}\text{N}$  shifts of the pyrazoles in the enzyme complex, the corresponding  $^{15}\text{N}$  chemical shifts of several pyrazole derivatives were determined (Table 2). The pyrazole-nicotinamide adduct (N-benzyl-1,4-dihydro-4-pyrazolylnicotinamide, V), which provides a model for the pyrazole- $\text{NAD}^+$  adduct, was prepared by addition of sodium hydroxide to a mixture of pyrazole and N-benzylpyridinium chloride (VI). This adduct has been reported by Angelis to be the C4 addition product and to have a half-life of about one hour at room temperature.<sup>29</sup>

We observed little decomposition at 7-8° during the ten hours required to obtain a natural-abundance spectrum. When the reaction conditions were altered as in Method B or C of the experimental section, more than one pyrazole derivative was formed, possibly due to polymerization or addition of pyrazole to C2 or C6 of the nicotinamide ring. The substances in these mixtures were too unstable to be isolated and were not characterized further. However, the ultraviolet absorption spectra of the product mixtures with maximum absorbances of about 320 nm are characteristic of 1,4-dihydronicotinamide derivatives (see Table 3). Any hydroxide-nicotinamide addition products present in the mixture would also affect the absorption spectra. Dittmer and Kolyer<sup>55</sup> have reported the formation of a 1,4-dihydronicotinamide product with a maximum absorbance of 330-335 nm, upon addition of sodium hydroxide to *N*-benzyl nicotinamidinium chloride, which they proposed to be a dimolecular ether, bridged at the 4-positions of the two dihydronicotinamide moieties.

The <sup>15</sup>N chemical shifts of products from each of the methods of carrying out the reaction are shown in Table 4.

Reaction products of pyrazole and nicotinamidinium ions are the only pyrazole derivatives for which the N1 chemical



Table 3. Ultraviolet Absorption Maxima of Dihydronicotinamide Derivatives.

Complexing Agent	Coenzyme or Coenzyme Analog	$\lambda_{\text{max}}(\text{nm})$ non-enzymic complex	$\lambda_{\text{max}}(\text{nm})$ LADH complex	solvent	Reference
Pyrazole	$\text{NAD}^+$	305	290	aqueous	24
	N-Benzyl- nicotinamidinium chloride	317 <sup>a</sup>	---	$\text{CHCl}_3$	29, this work
	N-Benzyl- nicotinamidinium chloride	318 <sup>b</sup>	---	$\text{CHCl}_3$	this work
	N-Benzyl- nikethamidinium chloride	321 <sup>c</sup>	---	$\text{CHCl}_3$	this work
	N-Methyl- nicotinamidinium chloride	315	---	aqueous	24
Imidazole	$\text{NAD}^+$	305	---	aqueous	28a
	N-Benzyl- nicotinamidinium chloride	315	---	aqueous	28a
Hydroxylamine	$\text{NAD}^+$	315	300	aqueous	28b
	N-Methyl- nicotinamidinium chloride	330	---	aqueous	24
Cyanide	$\text{NAD}^+$	325	310	aqueous	28b

- a Prepared by Method A (Experimental Section).
- b Prepared by Method B (Experimental Section).
- c Prepared by Method C (Experimental Section).

Table 4.  $^{15}\text{N}$  Chemical Shifts<sup>a</sup> of Reaction Products of  
 Pyrazole and N-Benzylnicotinamidinium Chloride VI or N-  
 Benzylnikethamidinium Chloride in Chloroform

Reactants	Method of Preparation <sup>b</sup>	$\delta^{15}\text{N}$		$^1J_{\text{NN}}(\text{H}_3)$
		N2	N1	
Pyrazole + VI	A	76.7	136.3	
$^{15}\text{N}$ -Labeled Pyrazole + VI	B			
Major products (~70% yield)		75.9	136.3	$12.7 \pm 1$
Minor products (~20% yield)		74.0	142.4	$13.7 \pm 1$
(~10% yield)		72.3	136.5	$12.7 \pm 1$
Pyrazole + N-Benzyl- nikethamidinium chloride	C			
(~50% yield)		76.6	138.1	
(~50% yield)		86.7	141.4	

a In parts per million upfield from external 1 M nitric acid in  $\text{D}_2\text{O}$ .

b See Experimental Section.

shifts have been found to be close to those of the enzyme complex. The N2 shift of the pyrazole-nicotinamide model adduct, as for all other pyrazole derivatives investigated, is considerably downfield from the N2 shift of the enzyme complex. The  $^{15}\text{N}$ - $^{15}\text{N}$  one-bond coupling constants for reaction products of  $^{15}\text{N}$ -labeled pyrazole and N-benzylpyridinium chloride were all about 13 Hz (see Table 4), similar to the  $^{15}\text{N}$ - $^{15}\text{N}$  one-bond coupling constant of about 10 Hz found for the LADH-NAD<sup>+</sup>-pyrazole complex.

#### Model Pyrazole-Zinc Complexes

The effects of complexation with zinc chloride on the chemical shifts of the nitrogens of pyrazole and some of its derivatives are summarized in Tables 5 and 6. The N-methylpyrazole (III)-zinc chloride adduct (IX) which we have prepared has the empirical formula of (N-methylpyrazole)<sub>2</sub>ZnCl<sub>2</sub> as determined by atomic analysis. The complex is insoluble in water, but soluble in chloroform and acetone. The pyrazole derivative, ethyl 2-pyrazolylethanoate (IV), was chosen as a model for zinc binding in the enzyme-inhibitor complex, because it was expected that the ester carbonyl group would enhance complexation of zinc chloride to N2 of the pyrazole ring.

Table 5.  $^{15}\text{N}$  Chemical Shifts<sup>a</sup> of Zinc Complexes of Pyrazole  
and Pyrazole Derivatives

Solute	Ratio <sup>d</sup>	Solvent	concn <sup>b</sup> <u>M</u>	$\delta^{15}\text{N}$		$\Delta \delta^{15}\text{N}^c$	
				N1	N2	N1	N2
Pyrazole + $\text{ZnCl}_2$	2:1	$\text{CH}_3\text{CN}$	3	148.2 <sup>e</sup>		(+44) <sup>f</sup>	
	1:1	$(\text{CH}_3)_2\text{SO}$	1	138.1 <sup>e</sup>		(+34) <sup>g</sup>	
$\text{N-Methylpyrazole}_2\text{ZnCl}_2$	2:1	$\text{CHCl}_3$	0.4	175.9	121.1	+1.3	+50.8
Ethyl 2-pyrazolyethanoate + $\text{ZnCl}_2$	2:1.5	$\text{CH}_3\text{CN}$	2	175.6	121.3	+2.3	+54.9

a In parts per million upfield from external 1 M nitric acid in  $\text{D}_2\text{O}$ .

b Concentration of pyrazole derivative.

c Change in chemical shift relative to uncomplexed compound (Table 2).

d Molar Ratio of pyrazole derivative to zinc chloride.

e Averaged nitrogen shift.

f Approximate change in shift based on change in average shift of +22.7 ppm.

g Approximate change in shift based on change in average shift of +17.7 ppm.

Table 6. Effects of Zinc Complexation on  $^{15}\text{N}$  Chemical Shifts<sup>a</sup> of 2 M Ethyl 2-Pyrazolyethanoate

solvent	ZnCl <sub>2</sub> , concn		$\delta^{15}\text{N}$		$\Delta \delta^{15}\text{N}^c$	
	M	Molar Ratio <sup>b</sup>	N2	N1	N2	N1
CH <sub>3</sub> CN	0	0	66.4	173.3	0	0
	1	2:1	117.9	175.3	+51.5	+2.0
	1.5	2:1.5	121.3	175.6	+54.9	+2.3
(CH <sub>3</sub> ) <sub>2</sub> SO	0	0	65.4	172.7	0	0
	2	2:1	87.3	174.2	+21.9	+1.5
	3	2:3	96.8	174.8	+31.4	+2.1
	4	2:4	104.9	175.4	+39.5	+2.7
	4.5	2:4.5	106.9	175.5	+41.5	+2.8

a In parts per million upfield from external 1 M nitric acid in D<sub>2</sub>O.

b Molar ratio of ethyl 2-pyrazolyethanoate to zinc chloride.

c Change in chemical shift relative to uncomplexed compound.

Complexing of IV with zinc chloride was found to be solvent-dependent. Dimethyl sulfoxide, which complexes well with zinc chloride, competes effectively with the pyrazole derivative for zinc, thus producing a smaller pyrazole N2 shift on saturation with zinc chloride (at a molar ratio of 2:4.5, IV:zinc chloride). Acetonitrile as solvent produced a larger pyrazole N2 shift than dimethyl sulfoxide on saturating a pyrazole solution with zinc chloride (2:1.5 molar ratio, IV:zinc chloride) than was observed at saturation with zinc chloride in dimethyl sulfoxide. Addition of smaller amounts of zinc chloride produced smaller shifts (Table 6). Only one pyrazole N2 resonance was observed in all cases, indicating fast exchange between complexed and uncomplexed states. For both solvents, the solubility of zinc chloride was many-fold higher in the presence of the pyrazole derivative than in neat solvent.

Other pyrazole derivatives were investigated for zinc-complexing ability, but either showed reduced complexation as exemplified by smaller changes in chemical shift or produced zinc complexes of too low solubility for  $^{15}\text{N}$  NMR spectra to be obtained. At saturation (1 M concentration zinc chloride) with zinc chloride of 2 M N-carbamoyl-3-methylpyrazole in dimethyl sulfoxide, the upfield shift of N1 was 0.5 ppm, while the upfield shift of N2 was only 0.4

ppm, relative to 3 M N-carbamoyl-3-methylpyrazole. This could be indicative of zinc complexation by the carboxamide group with little or no complexation by N2 of the pyrazole nucleus, or simply concentration effects, the pyrazole nitrogen shifts being affected by changes in the degree of intermolecular hydrogen bonding.

When neat ethyl 2-pyrazolyethanoate, (IV), is heated with 0.25 equivalents zinc chloride for 2 hours at 75°, the zinc chloride almost completely dissolves, producing a rose-colored solution similar to that of the ethyl 2-pyrazolyethanoate-zinc chloride complex in dimethyl sulfoxide. The N2 and N1 chemical shifts for this complex were found to be 88.8 and 175.0 ppm, respectively. The upfield shift change of about 20 ppm for N2 is a little less than half that found for addition of 0.5 equivalents zinc chloride to IV in acetonitrile.



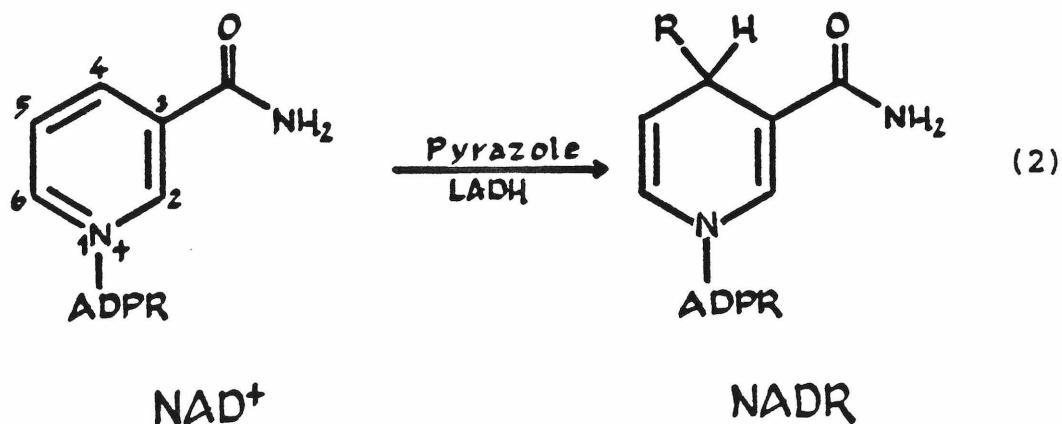
## DISCUSSION

I. Introduction

The  $^{15}\text{N}$  NMR spectra of the LADH- $\text{NAD}^+$ -pyrazole and LADH- $\text{NAD}^+$ -4-ethylpyrazole complexes are shown in Figures 4, 5 and 6. The assignment of resonances by analogy to the  $^{15}\text{N}$  resonances of other pyrazoles and NADH is unambiguous. This is the largest enzyme complex for which  $^{15}\text{N}$  spectra have so far been reported. The resonances are much sharper than might be predicted for a complex of MW greater than 80,000.

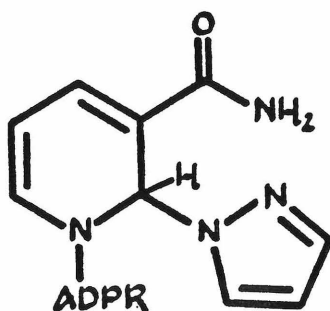
II. Coenzyme

The chemical shift of the nicotinamide ring nitrogen of the coenzyme in the ternary complex, 247.2 ppm, demonstrates that the coenzyme in the LADH- $\text{NAD}^+$ -pyrazole complex has the dihydro structure (Equation 2).

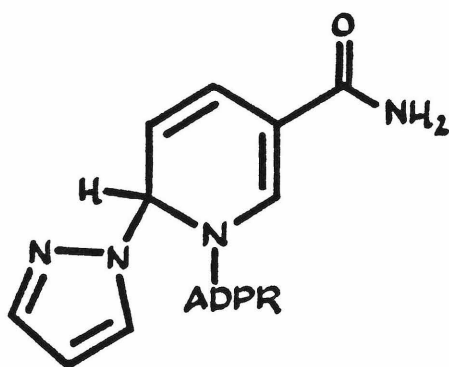


The upfield shift resulting from complex formation was 96 ppm relative to free  $\text{NAD}^+$ , and is comparable to the upfield change in shift in solution of 109 ppm that has been reported for reduction of  $\text{NAD}^+$  to  $\text{NADH}$ .<sup>50</sup>

The  $^{15}\text{N}$  chemical shift is wholly consistent with addition of pyrazole to C4 of the nicotinamide ring, as proposed by Theorell and Yonetani.<sup>24</sup> However, from the  $^{15}\text{N}$  shift of the nicotinamide N1 alone, it cannot be determined at which position addition has occurred. The resonance is 13 ppm downfield from that of  $\text{NADH}$  in solution, and it is possible that this is a large enough difference to indicate that addition has occurred at either C2 or C6. In which case, the  $^{15}\text{N}$ -labeled pyrazole N1 would be removed from the nicotinamide N1 by only one carbon atom (Figure 7), and the 13 ppm deshielding of the nicotinamide N1 would be attributable to the proximity of the electron-withdrawing pyrazole nucleus.



Product of C2 addition



Product of C6 addition

Figure 7. Other Possible Products of Pyrazole Addition to NAD<sup>+</sup>.

In all complexes studied so far, the conformation of bound coenzyme as determined by X-ray crystallography effectively rules out addition at C2, the nicotinamide ring being bound with the C6 side of the nicotinamide ring towards the substrate-binding region. Crystallographic studies<sup>9</sup> of the LADH-NAD<sup>+</sup>-pyrazole complex give a pyrazole N1-nicotinamide C4 bond distance of 2 Å, with N1-C6 distances being much greater. Clearly, considerable rearrangement of the crystalline active-site structure would be necessary to allow N1-C6 bond formation in solution.

Substitution of the C4 hydrogen of NADH by the more electronegative nitrogen of pyrazole might alone account for the downfield shift relative to NADH through a diamagnetic deshielding effect. <sup>13</sup>C NMR chemical shifts (Table 7) of the pyrazole-nicotinamide adduct V, and *N*-benzyl-1,4-dihydronicotinamide VII, as reported by Angelis,<sup>29</sup> demonstrate the deshielding effect of pyrazole substitution on the nicotinamide ring carbons, whose <sup>13</sup>C resonances are all shifted downfield in the pyrazole-nicotinamide adduct relative to *N*-benzyl-1,4-dihydronicotinamide. Steric and electronic effects of active-site residues probably also contribute to the shift difference, though their effect on NADH in the binary LADH-coenzyme complex has not been determined.

Table 7.  $^{13}\text{C}$  NMR Chemical Shifts<sup>a</sup> of the Model Pyrazole-NAD<sup>+</sup> Adduct, N-Benzyl-1,4-dihydro-4-pyrazolylnicotinamide V, and N-Benzyl-1,4-dihydronicotinamide VII.<sup>29</sup>

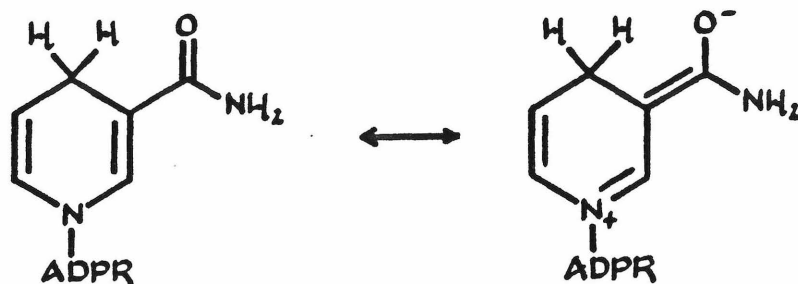
Carbon	V	VII	VII-V <sup>b</sup>
C2	139.2	139.0	- 0.2
C3	102.8	98.9	- 3.9
C4	54.8	22.7	-32.1
C5	106.8	103.2	- 3.6
C6	130.9	129.0	- 1.9
C7	169.5	170.3	+ 0.8

a In parts per million downfield from TMS.

b Negative values of VII-V indicate deshielding of V relative to VII.

Oppenheimer and Davidson<sup>50</sup> have found little or no solvent effect on the  $^{15}\text{N}$  chemical shifts of N1 of  $\text{NAD}^+$  and NADH. Their results indicate that the degree of hydrophobicity of residues surrounding the bound coenzyme should not exert much effect on the N1 chemical shift. There is, however, a large effect on the chemical shift, caused by a change of electronic state of N1 of nicotinamide derivatives, the resonance shifting about 100 ppm upfield upon formation of the dihydro derivative. Formally, N1 changes hybridization state from  $\text{sp}^2$  to  $\text{sp}^3$  with concurrent loss of aromaticity and charge upon dihydro derivative formation. However, Oppenheimer, Arnold and Kaplan<sup>56</sup> have proposed on the basis of proton NMR results that NADH in solution is in fast exchange between a conformation where the nicotinamide ring is planar and a conformation where the nicotinamide ring is puckered, but still planar at N1, equilibrium favoring the planar nicotinamide ring. Crystallographic studies<sup>57</sup> of *N*-benzyl-1,4-dihydronicotinamide have demonstrated that the ring is planar. The observation of absorption at 340 nm for NADH and at similar wavelengths for other dihydronicotinamide derivatives (see Table 3) again indicates planarity at N1, to allow the electronic transition to the resonance form (VIII) responsible for the absorption (Figure 8). The

hybridization state of N1 of the dihydronicotinamide ring can therefore be described as more  $sp^2$ -like than  $sp^3$ -like.



VIII

Figure 8. Resonance Forms of NADH.

It is possible that the coenzyme-binding region of the enzyme induces a change in the geometry of the nicotinamide moiety of the coenzyme upon binding. A 10-15 nm shift to shorter wavelength in the maximum absorbance of the absorption spectrum of dihydronicotinamide derivatives is seen upon binding to LADH (Table 3). This wavelength decrease corresponds to an increase in energy for the transition shown in Figure 8. This could conceivably be associated with a deviation from planarity by the nicotinamide ring. Cook, Oppenheimer and Cleland have proposed, on the basis of secondary isotope effects in the reaction of [N1- $^{15}\text{N}$ ]-labeled coenzyme and cyclohexanone or cyclohexanol with LADH,<sup>58</sup> that in the transition state, the

nicotinamide ring is bent into a boat-like conformation, facilitating the reaction by increasing the reactivity of C4. They suggest that this is brought about by a change in conformation of the enzyme. Binding of coenzyme does induce a conformational change,<sup>59</sup> and it has been shown that the amide group of the nicotinamide ring is necessary for this change to occur.<sup>60</sup> Both LADH-NADH-dimethyl sulfoxide<sup>8</sup> and LADH-NAD<sup>+</sup>-pyrazole<sup>9</sup> complexes crystallize in triclinic form, with approximately the same enzyme conformation, which is different from the uncomplexed LADH or LADH-ADPR conformations. In these crystalline complexes, the nicotinamide ring of the coenzyme is planar. If the LADH-NAD<sup>+</sup>-pyrazole complex may be viewed as a transition-state analog, the crystallographic determination of the geometry of the nicotinamide ring disproves the proposal by Cook and coworkers that the transition state involves a pyramidal nicotinamide N1.

The <sup>15</sup>N chemical shifts reported here for the ternary complex in solution also do not support this hypothesis, the nicotinamide chemical shift being close to that of dihydronicotinamides in solution, but shifted in the direction of less shielding. An increase in the p-character of N1 as caused by deviation from planarity to produce a pyramidal N1 should cause an increase in shielding, i.e., an



upfield shift, because of decreases in lone-pair delocalization.

The nicotinamide nitrogen chemical shift thus indicates that the state of the coenzyme in the LADH-NAD<sup>+</sup>-pyrazole complex in solution is similar to that found in the crystalline complex.<sup>9</sup> Together with the N1 pyrazole chemical shifts, which will be discussed later, these results demonstrate that in the active site of the enzyme, pyrazole adds to the nicotinamide ring of the coenzyme, producing the dihydronicotinamide form of the coenzyme.

### III. Pyrazole

#### III.1. Introduction

Pyrazole is a five-membered aromatic heterocycle with two adjacent ring nitrogens (structure I). The chemistry of pyrazoles has been reviewed by Kost and Grandberg.<sup>61</sup> The pyrazole nucleus is generally quite stable. Much of the chemistry of pyrazole concerns reactions involving the labile N-H bond. The hydrogen at N1 is easily replaced by various substituents, producing N-substituted pyrazole derivatives.

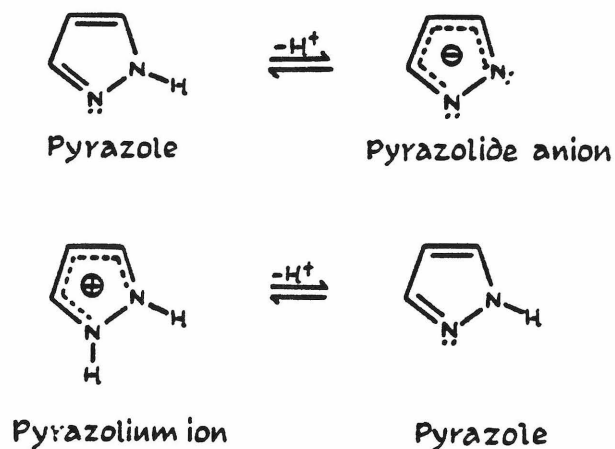


Figure 9. Acid-Base Behavior of Pyrazole

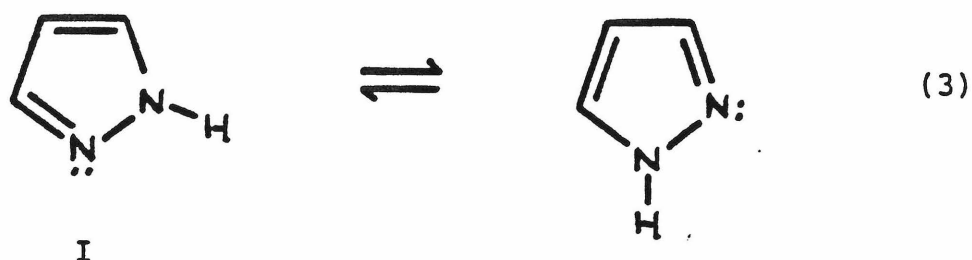
The presence of two types of nitrogens, one pyrrole-type, N1, and one pyridine-type, N2, explains the amphoteric behavior of pyrazole. Neutral pyrazole loses a proton to form the pyrazolide anion, as in Figure 9, with a  $pK_a$  greater than 14.<sup>62</sup> The protonated form of pyrazole, the pyrazolium ion, loses a proton as in Figure 9, with a  $pK_a$  of 2.5.

The solubility of pyrazole in most solvents is quite high. This has allowed the  $^{15}\text{N}$  NMR of pyrazoles to be studied at the natural-abundance level. However, the solubility of LADH complexes is on the millimolar level, making natural-abundance  $^{15}\text{N}$  NMR studies of inhibitor bound

to LADH infeasible. However, the ready availability of  $^{15}\text{N}$ -labeled hydrazine permits facile preparation of doubly- $^{15}\text{N}$ -labeled pyrazole and pyrazole derivatives and NMR spectra of  $^{15}\text{N}$ -labeled pyrazoles may be obtained at millimolar concentrations. The result is that it is quite feasible to make  $^{15}\text{N}$  studies of the LADH- $\text{NAD}^+$ - $^{15}\text{N}$ -labeled pyrazole complex.

### III.2. $^{15}\text{N}$ NMR of Pyrazole

$^{15}\text{N}$  chemical shifts of several pyrazoles are given in Table 2. Pyrazole (I), in aqueous solution gives rise to a single  $^{15}\text{N}$  resonance. This is the result of a fast tautomeric equilibration involving the pyrrole-type, N1, and the pyridine-type, N2, nitrogens as illustrated in equation 3.



Under conditions where the exchange of the proton between the two nitrogens is fast on the NMR time scale, only one average resonance is observed. The chemical shift of this resonance is the average of the individual shifts for the

two tautomers. The averaging process is not quite complete because addition of a small amount of base or acid can sharpen the resonance, by catalyzing tautomeric equilibration.

The exchange rate between the two tautomers is approaching a rate which is intermediate on the NMR time scale when exchange broadening occurs, and should be comparable to  $2\pi$  times the shift difference in Hertz, where the shift difference in Hertz is the frequency of the spectrometer times the shift difference between the two nitrogen resonances in the absence of exchange. This shift difference is 92 ppm, based on the shifts of the two nitrogens in dimethyl sulfoxide (Table 2). The rate of tautomeric equilibration in aqueous solution where exchange broadening is occurring is thus on the order of  $1.1 \times 10^4 \text{ sec}^{-1}$ .

Pyrazole in dimethyl sulfoxide solution gives rise to two separate, broad  $^{15}\text{N}$  resonances because in this solvent tautomeric equilibration is slow. In acetonitrile solution, it is sometimes difficult to obtain any signal at all from samples 1-2 M in concentration, an indication of intermediate exchange rates, with the resonances so broadened as to be indistinguishable from the baseline. A broad averaged signal was obtained from a 5 M solution of

pyrazole in acetonitrile (Table 2). Here, tautomeric equilibration was clearly accelerated, perhaps by a concentration-dependent increase in intermolecular proton transfer or by traces of water in the sample.

Protonation and hydrogen bonding effects on the chemical shift of pyrazole derivatives have been investigated by Schuster, Dyllick-Brenzinger and Roberts.<sup>54</sup> Protonation of pyrazole to form the pyrazolium ion causes an upfield shift of 45.9 ppm for the averaged nitrogens. The effect of protonation of N2 on the individual nitrogen resonances is seen in N-substituted pyrazoles. Substitution at N1 prevents tautomeric equilibration of the two nitrogens of the pyrazole nucleus. Thus, individual resonances for the two non-equivalent nitrogens can be obtained for N-substituted pyrazoles even in aqueous solution. Protonation of N-methylpyrazole results in a 100-ppm upfield shift of N2, because of the removal of the paramagnetic deshielding associated with the  $n \rightarrow \pi^*$  transition in the neutral compound. Protonation affects the N1 chemical shift to a much lesser degree, there being an upfield shift of 4 ppm.

Increases in hydrogen bonding cause substantial upfield shifts of N2 as well as small upfield shifts of N1. The maximum shift associated with hydrogen bonding of N2 of pyrazole derivatives may be approximated by the shift of

+17.9 ppm for N2 of N-methylpyrazole upon change of solvent from chloroform to trifluoroethanol. Here, the corresponding change in the N1 resonance is upfield by 1.4 ppm.<sup>54</sup>

Deprotonation of neutral pyrazole to form the pyrazolide anion causes a downfield shift in the averaged resonance. The chemical shift of pyrazole decreases upon increase of pH above pH 12, to a value of 80 ppm at pH 15.2, consistent with a  $pK_a$  of greater than 13.7, as determined by titrations by Kanamori.<sup>63</sup> This downfield shift is caused by an increase in the paramagnetic deshielding of N1 upon loss of the proton. The most downfield  $^{15}\text{N}$  shift so far observed for a pyrazole derivative is 55.1 ppm, found for 5 mM  $^{15}\text{N}$ -labeled pyrazole in dimethyl sulfoxide after addition of excess sodium hydride. It was not determined whether this averaged signal was the result of fast proton exchange between the pyrazolide anion and any neutral pyrazole still present in solution as the result of incomplete anion formation.

### III.3. $^{15}\text{N}$ Chemical Shifts of Model N-Substituted Pyrazoles

The  $^{15}\text{N}$  chemical shifts of various pyrazole derivatives (Table 2) were determined for comparison with the enzyme

complex. The chemical shift of the pyrrole-type nitrogen N1 of pyrazole derivatives depends considerably on the nature of the N1 substituent. All N-substituted pyrazole derivatives stable at room temperature which were investigated have N1 shifts greater than 150 ppm, the most shielded being that of N-methylpyrazole at 174.6 ppm, which has the electron-releasing methyl group as a substituent. The N1 chemical shifts of derivatives with the strongly electron-withdrawing substituents,  $-\text{CONH}_2$ , and  $-\text{CH}_2\text{OH}$ , were the most downfield, at 152.6 and 156.6 ppm, respectively, in dimethyl sulfoxide, but were still more than 10 ppm upfield from the N1 chemical shifts of the LADH-NAD<sup>+</sup>-pyrazole complex.

The only pyrazole derivatives found so far that have N1 chemical shifts close to that found for the enzyme ternary complex are the pyrazole-nicotinamidinium ion reaction products (Table 4). N-Benzyl-1,4-dihydro-4-pyrazolyl nicotinamide (V) was prepared to serve as a model for the pyrazole-NAD<sup>+</sup> adduct of the enzyme inhibitor complex. Angelis has reported that in this adduct, the site of addition of pyrazole to nicotinamide is at C4. The N1 chemical shift for this adduct, 136.3 ppm in chloroform, is 5.8 ppm downfield from that of the LADH-NAD<sup>+</sup>-pyrazole complex, indicating that the dihydronicotinamide moiety has

## Model Pyrazole-NAD<sup>+</sup> Adduct

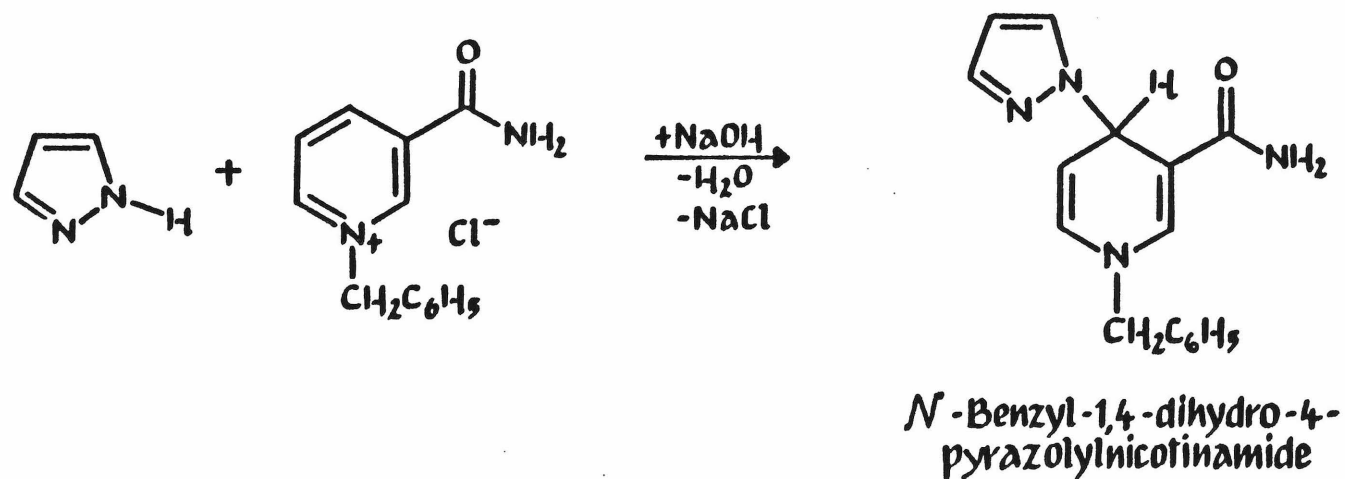


Figure 10. Formation of the Model Pyrazole-NAD<sup>+</sup> Adduct.



a much larger deshielding effect than the other N1 substituents investigated. The model pyrazole-NAD<sup>+</sup> adduct V was prepared by the method of Angelis<sup>29</sup> by the addition of base to an equimolar mixture of pyrazole and N-benzylnicotinamidinium chloride in water (Figure 10). The chemical shifts of the pyrazole nitrogens of this compound provide a good point of reference for the interpretation of the chemical shifts of the enzyme complex. The fact that N1 is unusually deshielded compared to other pyrazole derivatives may be attributed to the particular effect of the dihydronicotinamide moiety, as evidenced by the chemical shifts of other pyrazole-nicotinamide complexes. When the reaction conditions for pyrazole addition to N-benzylnicotinamidinium chloride are altered (see Experimental Section), other minor (about 30% yield), as yet unidentified, pyrazole derivatives are formed. These pyrazole-nicotinamide reaction products have nitrogen shifts close to those of V (see Table 4). These may be the products of C2 and C6 addition of pyrazole to the nicotinamide ring or of polymerization. Addition of hydroxide to N-benzylnicotinamidinium chloride results in the formation of dimers and trimers of N-benzyl-dihydronicotinamide.<sup>55,64</sup> This suggests that polymers of N-benzyl-1,4-dihydro-4-pyrazolynicotinamide may also be

formed, with structures similar to those proposed for the hydroxide polymerization products, that is, where the dihydronicotinamide rings are bridged through C2, C4 or C6 and the amide nitrogen or the benzyl methylene carbon. Because both the N1 and N2 chemical shifts are similar to V and the N1 chemical shifts are considerably different from other pyrazole derivatives with the exception of the enzyme complex, it may be assumed that these chemical shifts are characteristic of dihydronicotinamide substitution at N1 of the pyrazole ring.

The chemical shifts of the pyridine-type N2 nitrogens of pyrazole derivatives in non-hydrogen-bonding solvents were found to be in the range of 65.4-76.7 ppm, with the exception of N-carbamoyl-3-methylpyrazole. The N2 chemical shift of this derivative, 81.2 ppm, is more shielded than the others, possibly because of intermolecular hydrogen bonding between N2 and the amide  $\text{-NH}_2$  group of the substituent in the fairly concentrated (3 M) solution used for the chemical-shift determinations.

The N2 resonance of the model pyrazole- $\text{NAD}^+$  adduct, V, is the most upfield of those found for the other pyrazole derivatives, yet it is 41.1 ppm downfield from N2 of the enzyme ternary complex. This shift difference seems much larger than can be attributed to hydrogen bonding (about 18

ppm<sup>54</sup>) and strongly suggests complexation of N2 of pyrazole in the enzyme complex by the active-site zinc.

#### III.4 <sup>15</sup>N Chemical Shifts of Model Pyrazole-Zinc Complexes

The effects of metal complexation on the <sup>15</sup>N chemical shifts of pyrazole compounds have not previously been reported, but there are accounts of the effect of zinc complexation on the <sup>15</sup>N chemical shifts of the pyridine-type nitrogens of other compounds.

Alei and coworkers have investigated zinc-complexation effects on the chemical shift of the pyridine-type N3 nitrogen of imidazole<sup>65</sup> and N-methylimidazole<sup>66</sup> in aqueous solution. They found an upfield shift of 11-17 ppm for the averaged nitrogen resonances of zinc-complexed imidazole, which is less than half that due to protonation. The actual effect on N3 is difficult to determine because of fast tautomeric exchange of the two nitrogens. However, this average shift may be interpreted as 25-40 ppm upfield shift of the pyridine-type nitrogen upon zinc complexation, by analogy to N-methylimidazole, whose N3 nitrogen on zinc complexation moves upfield by +35-40 ppm. This is about half the shift, +73 ppm, caused by protonation of N3. The N1 resonance was found to shift downfield by 3-5 ppm.

The effect of zinc complexation on the  $^{15}\text{N}$  chemical shifts of several nucleosides at natural abundance, was investigated by Buchanan and Stothers.<sup>67</sup> The observed  $^{15}\text{N}$  resonances were most likely averaged resonances of uncomplexed nucleoside and two or more forms of zinc-complexed nucleoside, and therefore the shifts were by no means surely the maximum possible on full zinc complexation.

On addition of equimolar zinc nitrate to 0.5 M adenosine in dimethyl sulfoxide, the N7 resonance shifted upfield 7.5 ppm relative to uncomplexed adenosine. The N1 resonance shifted 1.6 ppm upfield, which indicates a lesser degree of zinc complexation to N1 than N7. Protonation of N1 results in a 72.6 ppm upfield shift of N1. These results suggest that the major site of zinc complexation of adenosine is N7, as illustrated in Figure 11(a), even though protonation occurs at N1.

On addition of equimolar zinc nitrate to 0.75 M cytidine in dimethyl sulfoxide, N3 was observed to shift upfield 22 ppm, while N1 shifted upfield only 2 ppm. Here, the major site of zinc complexation is N3, with lesser complexation to N1. This is similar to what is observed on protonation, which also occurs at N3, but the protonation shift is +64.8 ppm for N3. The larger upfield shifts for

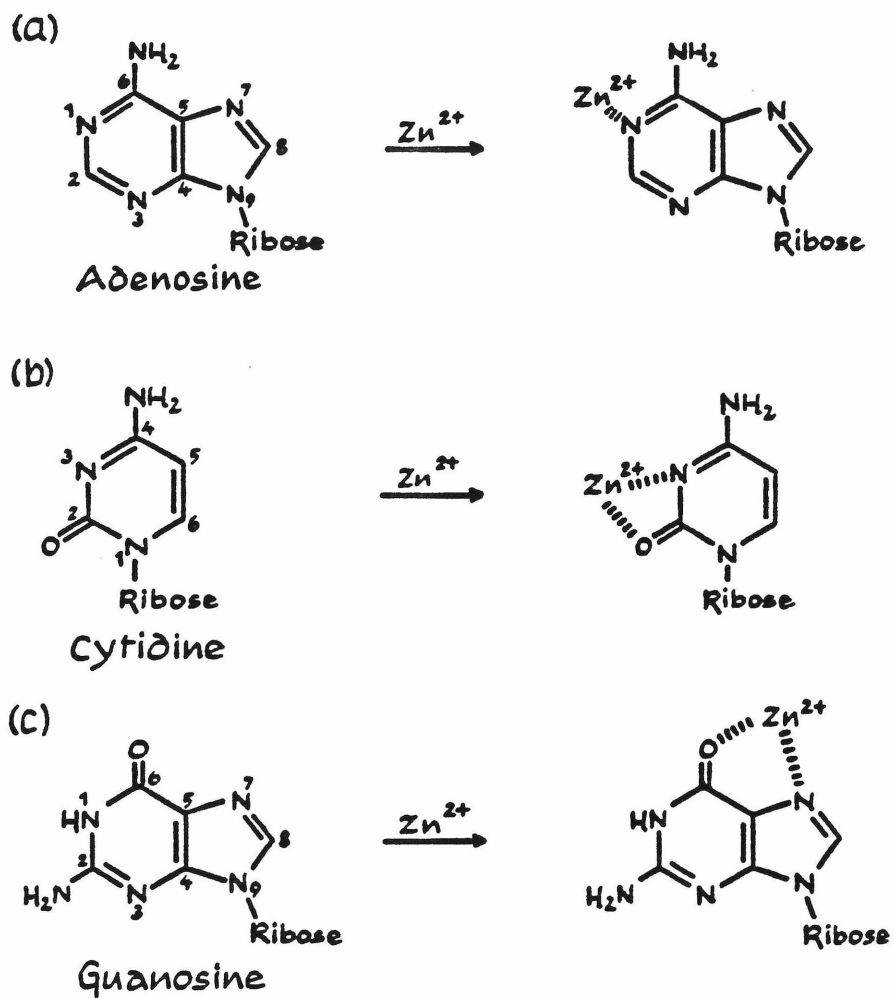


Figure 11. Proposed Sites of Zinc Complexation of Several Nucleosides.<sup>67</sup> (a) Zinc complex of adenosine. (b) Zinc complex of cytidine. (c) Zinc complex of guanosine.

cytidine than for adenosine speak for fuller zinc complexation as the result of stabilization of the N3-zinc complex by simultaneous coordination to the carbonyl group, as illustrated in Figure 11(b). The effect of zinc complexation on the  $^{15}\text{N}$  chemical shifts of guanosine was similar to that found for cytidine, which indicates the major site of zinc complexation to be at N7, probably bidentate with the carbonyl as illustrated in Figure 11(c).<sup>67</sup>

Happes and Morales<sup>68</sup> determined the  $^{15}\text{N}$  shifts caused by zinc complexation of adenosine 5'-triphosphate, ATP, in  $\text{D}_2\text{O}$  solution. N7 was found to shift upfield 3 ppm upon addition of equimolar zinc chloride. This is a much smaller shift than that found for adenosine by Buchanan and Stothers,<sup>67</sup> but indicates a similar complexation of zinc to N7.

Based on these reports of the effects of zinc-complexation on the  $^{15}\text{N}$  chemical shifts of pyridine-type nitrogens (up to +40 ppm changes), it could be predicted that N2 of pyrazole and its derivatives would shift upfield upon complexation to zinc. However, the magnitude of the shift arising from full zinc complexation could hardly be predicted. The magnitude is very important, so that the full complexation shift may be compared to the shift

demonstrated by the enzyme complex and allow the extent of direct zinc complexation in the enzyme complex to be determined.

The  $^{15}\text{N}$  chemical shifts of various model pyrazole-zinc complexes are collected in Table 5. Zinc complexation of N2 (the pyridine-type nitrogen) of pyrazole as expected causes an upfield shift, just as does protonation of N2. The reason is that coordination to zinc (or a proton) greatly decreases the paramagnetic deshielding which can be ascribed to an increase in the mixing in of excited states into the ground state corresponding to the  $n \rightarrow \pi^*$  transition of neutral pyrazole when the pyrazole is placed in a magnetic field. Complexing of the  $n$  electrons with zinc or a proton should cause the energy of this transition to increase and hence reduce the magnitude of the paramagnetic shielding.

The maximum complexation shifts were demonstrated by the N-methylpyrazole (III)-zinc chloride complex IX dissolved in chloroform and the ethyl 2-pyrazolyethanoate (IV)-zinc chloride complex X in acetonitrile. These N2-zinc shifts, +50.8 and +54.9 ppm, respectively, are probably close to the shifts due to complete zinc complexation, as will be discussed later. However, the observed resonances may be in fact the averaged N2 resonances of complexed and uncomplexed pyrazole derivatives. It is therefore important

to subject the shifts of these model pyrazole-zinc complexes to close scrutiny before designating them to be those which correspond to full zinc complexation.

While one might expect the upfield shift upon zinc complexation of a pyrazole N2 to be close to the reported protonation shifts, on the order of 100 ppm,<sup>54</sup> the zinc complexation shifts of III and IV are about half that. Nee and Roberts<sup>69</sup> report upfield shifts upon complexation of guanosine and cytidine by cis-diammine-dichloroplatinum which were greater than the respective protonation shifts. However, the effect of platinum with its low-lying d orbitals in these square planar complexes is probably very different from the effect of zinc in the model pyrazole-zinc complexes. For pyridine-type nitrogens similar to N2 of pyrazole, all evidence supports the conclusion that zinc-complexation shifts are about half the protonation shifts, though in the same direction. Alei and coworkers found this to be the case for zinc complexation of N-methylimidazole, where the zinc complexation shift of N3 is +35-40 ppm and the protonation shift is +73 ppm.<sup>66</sup>

The stoichiometry of complexation, the extent of exchange between complexed and uncomplexed pyrazole, and the geometry of the complex should all affect the magnitude of the shielding caused by zinc complexation.



The number of pyrazoles per zinc in the crystalline N-methylpyrazole-zinc chloride complex has been determined by atomic analysis to be two, the compound having been isolated before obtaining the  $^{15}\text{N}$  spectrum in chloroform. The coordination number of ethyl 2-pyrazolyethanoate to zinc in acetonitrile solution is not known. However, on the basis of the molar ratio of IV to zinc chloride at saturation, 2:1.5, and on the assumption that ethyl 2-pyrazolyethanoate coordinates as a bidentate ligand as in Figure 12, it is expected that both IV-zinc and  $\text{IV}_2$ -zinc complexes exist. The argument is that almost all the zinc chloride present must exist as ethyl 2-pyrazolyethanoate complexes, because the solubility of zinc chloride in neat acetonitrile is low. (If indeed the ester carbonyl group alone coordinates to zinc, the existence of the  $\text{IV}_2$ -zinc complex is not required to explain the stoichiometry of the system.) The IV-zinc and  $\text{IV}_2$ -zinc complexes must be in fast exchange because only one averaged  $\text{N}_2$  signal is observed. The actual shift difference between the two proposed IV complexes is not known. Alei and coworkers<sup>65</sup> have estimated shift differences of up to about 10 ppm for imidazole-zinc complexes of varying stoichiometries in aqueous solution.

The extent of exchange is hard to determine by NMR techniques if the exchange is fast on the NMR time scale,

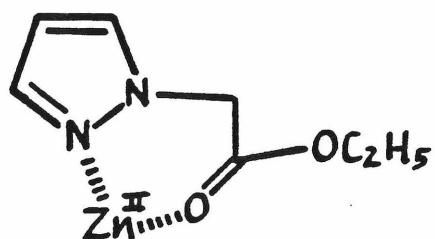


Figure 12. Proposed Sites of Zinc Complexation of Ethyl 2-Pyrazolylethanoate (IV).

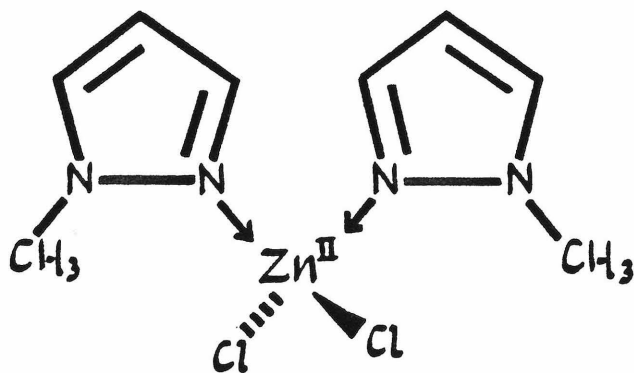


Figure 13. Proposed Structure of the *N*-Methylpyrazole-Zinc Chloride Complex IX, (N-Methylpyrazole)<sub>2</sub>ZnCl<sub>2</sub>.

resulting in one average N2 resonance. Only one N2 resonance is observed for each model system, indicating either fast exchange or slow exchange where the concentration of the uncomplexed species is too low to be observed. In the N-methylpyrazole-zinc chloride complex IX, the extent of ligand exchange in chloroform solution is expected to be slight, if at all, because of the poor ability of chloroform to solvate zinc chloride and the shift observed for N2 of the N-methylpyrazole-zinc chloride complex should be that of the fully complexed nitrogen.

The extent of exchange in the ethyl 2-pyrazolyethanoate (IV)-zinc chloride systems in acetonitrile and dimethyl sulfoxide solutions is not as easy to estimate. Acetonitrile and particularly dimethyl sulfoxide generally have much greater coordinating and ionizing abilities for cations than chloroform. While dissociation of pyrazole-zinc complexes has been found<sup>70</sup> to be generally low in acetonitrile, it occurs sufficiently in the IV-zinc system to allow signal averaging of the complexed and uncomplexed nitrogens. Evidence for this is the observation, on addition of zinc chloride to produce a 2:1 molar ratio of IV:zinc chloride, of one N2 resonance for IV in acetonitrile, which shifts upfield upon further addition of zinc chloride. However, the resonance observed

on addition of zinc chloride to produce a 2:1.5 molar ratio may be at the position of fully complexed N2. At this saturating zinc chloride concentration, only a +2.6 ppm change in shift of N2 is seen compared to the shift observed at a 2:1 molar ratio. The contribution of N2 of uncomplexed IV to the observed shift is expected to be slight.

In dimethyl sulfoxide solution, however, the case is different. The solubility of zinc chloride in neat dimethyl sulfoxide is much greater than in neat acetonitrile, where prior addition of pyrazole is necessary to obtain appreciable zinc chloride concentrations. Dimethyl sulfoxide is a good zinc-coordinating agent,<sup>71</sup> effectively competing with pyrazole for zinc. The maximum shift observed for the zinc complex of ethyl 2-pyrazolyethanoate, +41.5 ppm, is 13.4 ppm less than that observed in acetonitrile. In dimethyl sulfoxide, again a single N2 resonance is observed which is expected to be the weighted average resonance for N2 of complexed and uncomplexed pyrazole derivative. This resonance shifts upfield on further addition of zinc chloride. To reach saturation of zinc chloride, at least 4.5 moles of zinc chloride must be added to a 2 M solution of IV. As seen from the data in Table 6, the change in shift of N2 upon addition of zinc chloride has begun to level off at the molar ratio of 2:4.5

(IV:zinc chloride). However, because of the contribution of uncomplexed IV to the observed chemical shift and because of the high degree of participation of solvent in the complexation of the zinc, the IV-zinc chloride complex in dimethylsulfoxide is not likely to be a good model system for a fully complexed pyrazole and will not be used for comparison to the enzyme complex.

The geometry of the *N*-methylpyrazole-zinc chloride complex in chloroform, in the absence of coordination of solvent to zinc, is most likely tetrahedral, the proposed geometry of crystalline (pyrazole)<sub>2</sub>ZnCl<sub>2</sub>,<sup>72</sup> as illustrated in Figure 13, the solvent molecules being unable to coordinate to the metal. This is the expected geometry of the LADH-NAD<sup>+</sup>-pyrazole complex. If both the pyrazole nitrogen and the ester carbonyl coordinate to the zinc, the geometry of the proposed (ethyl 2-pyrazolyethanoate)<sub>2</sub>-ZnCl<sub>2</sub> (IV<sub>2</sub>-zinc) complex in acetonitrile should be octahedral, the preferred geometry of six-coordinate Zn<sup>II</sup>, the chloride ions not dissociating much in acetonitrile. The four-coordinate crystalline Co<sup>II</sup> complex (*N*-carbamoylpyrazole)CoCl<sub>2</sub> is proposed to be a tetrahedral complex.<sup>73</sup> Similarly, the mono IV-zinc complex in acetonitrile in the absence of solvent coordination should be tetrahedral. Acetonitrile is able to coordinate to zinc, as demonstrated by the conductance of

zinc perchlorate in acetonitrile.<sup>74</sup> However, in the IV-zinc system in acetonitrile, it is not known to what extent solvent coordination occurs.

### III.5. $^{15}\text{N}$ Chemical Shifts of the Enzyme Ternary Complexes

#### LADH-NAD<sup>+</sup>-Pyrazole

The chemical shift of the pyrrole-type nitrogen, N1, of pyrazole in the LADH-NAD<sup>+</sup>-pyrazole complex is 142.1 ppm (Table 1). This is considerably downfield from N1 resonances of identified pyrazole derivatives (Table 2) other than the pyrazole-NAD<sup>+</sup> model adduct, N-benzyl-1,4-dihydro-4-pyrazolynicotinamide, V, which has an N1 resonance of 136.3 ppm. As discussed earlier, the N1 shift of V seems characteristic of binding to dihydronicotinamide. Therefore, the N1 shift of the LADH-NAD<sup>+</sup>-pyrazole complex is indicative of pyrazole N1-nicotinamide complex formation within the active site of the enzyme through pyrazole addition to the nicotinamide ring.

The site of addition of pyrazole to the nicotinamide ring in V has been reported by Angelis to be C4.<sup>29</sup> Our NMR shifts of the ternary complex cannot be used to unambiguously assign the position where pyrazole binds to the nicotinamide ring. Other unidentified, minor (about 30% of the total) reaction products of pyrazole and N-benzylpyridinium chloride have N1 chemical shifts (Table 4) similar to those of the model pyrazole-NAD<sup>+</sup> adduct V and the enzyme ternary complex. While these products with

similar N1 shifts may be the result of polymerization of V, they could also be the result of C2 or C6 addition to the nicotinamide ring. However, X-ray crystallographic studies of the LADH-NAD<sup>+</sup>-pyrazole complex demonstrate bond formation between N1 of pyrazole and C4 of the nicotinamide ring.<sup>9</sup>

The pyrazole N1 chemical shift found for the enzyme complex is 5.8 ppm upfield from that found for the model adduct, probably because of the effect of a change in the substituent at the nicotinamide nitrogen and/or the effect of interaction with enzyme residues. The effect of ribosyl substitution versus benzyl substitution at the nicotinamide nitrogen may be seen from a comparison of the <sup>13</sup>C chemical shifts of NADH<sup>75</sup> and N-benzyl-1,4-dihydronicotinamide.<sup>29</sup> The C4 resonance of NADH is shielded by 0.8 ppm relative to C4 of N-benzyl-1,4-dihydronicotinamide. The N1 chemical shift of pyrazole attached to C4 of the coenzyme should therefore be shielded with respect to that of pyrazole attached to C4 of the benzyldihydronicotinamide moiety, as actually occurs in the enzyme complex. Also contributing to the +5.8 ppm discrepancy could be the effects of a N1-C4-nicotinamide ring bond angle and bond distance in the enzyme complex which differ significantly from the model adduct because of constraints imposed by the active-site residues. Eklund and coworkers<sup>9</sup> report a N1-C4-nicotinamide ring bond



angle of about  $90^\circ$  and a N1-C4 bond distance of 2 Å for the crystal structure of LADH-NAD<sup>+</sup>-pyrazole determined at 2.9 Å resolution. Both of these differ from that expected for the adduct in solution. The bond angle would be expected to be close to the tetrahedral value of  $109.5^\circ$  and the bond distance much shorter, by about 0.5 Å.

The pyridine-type nitrogen, N2, of pyrazole in the ternary complex has a chemical shift of 117.8 ppm (Table 1). This is 40-50 ppm upfield from the N2 chemical shifts of other pyrazoles in the absence of hydrogen bonding (Table 2), 41.1 ppm upfield from that of the pyrazole-NAD<sup>+</sup> model adduct V (Table 1). The maximum upfield shift which can reasonably be ascribed to hydrogen bonding is about 18 ppm, based on the change in shift of +17.9 ppm for N2 of N-methylpyrazole upon change of solvent from chloroform to trifluoroethanol.<sup>54</sup> The only reasonable explanation for the more than 40 ppm shielding of the pyrazole N2 in the ternary complex relative to the model adduct is substantial complexation by the active-site zinc.

Evidence in support of zinc complexation of pyrazole in the ternary enzyme complex is provided by the shift changes upon zinc complexation of N-methylpyrazole, III, and ethyl 2-pyrazolylolethanoate, IV, 50.8 and 54.9 ppm upfield, respectively, for the N2 resonances in chloroform and

acetonitrile, respectively. The N2 shift changes of these model pyrazole-zinc complexes, (N-methylpyrazole)<sub>2</sub>ZnCl<sub>2</sub> (IX, Figure 12) and the ethyl 2-pyrazolylethanoate-zinc complex (X, Figure 13) were the largest for various pyrazole-derivative zinc complexes investigated (Table 5). (The instability of the model pyrazole-NAD<sup>+</sup> adduct V in the presence of metal ions,<sup>29</sup> was such that the effect of zinc complexation on its N2 chemical shift could not be determined.)

The magnitude of the zinc complexation shift should be affected by the nature of the other ligands to zinc in the complex. In the enzyme, there are one histidine and two cysteine ligands to the catalytic zinc ion, which leaves a fourth coordination site open for complexation of solvent, substrate, or inhibitor. Among the model compounds, the second pyrazole in the N-methylpyrazole-zinc chloride adduct is an analog for the histidine residue, and chloride ion, a strongly associated ligand in non-nucleophilic solvents such as chloroform, is an analog for the cysteine residues. With the ethyl 2-pyrazolylethanoate-zinc chloride complex, dissolved in acetonitrile, the ester carbonyl group of ethyl 2-pyrazolylethanoate may, or may not, be as good an analog for histidine as pyrazole. Furthermore, there could well be competition between chloride ion and acetonitrile for the

third and fourth ligand sites. Intuitively, the +50.8 ppm  $^{15}\text{N}$ -complexation shift for the N-methylpyrazole-zinc complex could be a better estimate for the shift upon full zinc complexation than the +54.9 ppm for the ethyl 2-pyrazolyethanoate-zinc complex. However, no definitive judgment can be made at this time.

It is possible that in the LADH- $\text{NAD}^+$ -pyrazole complex there is fast exchange between a state where N2 of pyrazole is directly coordinated to zinc and a state where water or hydroxide ion is complexed to zinc and hydrogen bonded to N2 of pyrazole, in effect, an inner sphere-outer sphere equilibration process. As will be discussed later, the linewidths of the observed nitrogens of the enzyme complex are narrow, in agreement with a high degree of mobility of the pyrazole moiety. If one takes the full zinc complexation shift to be 51-55 ppm, and the hydrogen-bonding shift to be 18 ppm, the +41 ppm N2 shift of the enzyme complex relative to the model adduct V indicates that the inner-sphere state contributes 60-70% to the whole. However, it should be noted that this range of values approximates the lower limit of inner-sphere coordination of pyrazole to zinc in the ternary complex, and that it is possible that the +41 ppm N2 shift corresponds to full inner-sphere complexation.

If there is 100% inner-sphere coordination of pyrazole in the enzyme complex in solution, as in the crystalline complex,<sup>9</sup> the fact that the zinc complexation shift determined for the enzyme is 10-14 ppm less than that determined for the model complexes could be attributed to differences in the nature of the ligands and the steric requirements of residues in the active site, as well as the nature of the substituent at N1.

#### LADH-NAD<sup>+</sup>-4-Ethylpyrazole

The LADH-NAD<sup>+</sup>-4-ethylpyrazole complex was prepared to determine the effect that tighter binding of inhibitor has on the N1 and N2 resonances of the pyrazole nucleus. The inhibition constant in the presence of NAD<sup>+</sup> of 4-ethylpyrazole, structure II, is almost 30 times smaller than that of pyrazole ( $K_I=0.007$  and  $0.2 \mu\text{M}$ , respectively). Alkyl substituents at the 4-position increase the stability of pyrazole-inhibitor complexes because of interactions between the substituent and the hydrophobic cleft of the substrate-binding region of the enzyme. While the substrate complex containing the 4-iodopyrazole ( $K_I=0.02 \mu\text{M}$ <sup>27</sup>) was found by X-ray crystallography to have a structure which is very similar to that of the complex containing pyrazole itself, these hydrophobic interactions may lead to a

conformation of the pyrazole nucleus in the 4-ethylpyrazole complex which differs from that of the pyrazole complex. The N1 chemical shift of the ternary complex should reflect changes in the N1-C4 bond distance and angle to the nicotinamide ring. The N2 chemical shift should be affected by changes in the N2-zinc bond distance and changes in the inner sphere-outer sphere equilibrium, if any.

Our  $^{15}\text{N}$  shifts indicate that the structure of the LADH-NAD $^{+}$ -4-ethylpyrazole complex is very similar to that of the LADH-NAD $^{+}$ -pyrazole complex (Table 1). The N1 chemical shift in the 4-ethylpyrazole complex, 146.0 ppm, is 3.9 ppm upfield from that of the pyrazole complex, possibly as the result of substitution at the 4-position of pyrazole and of small changes in geometry about the N1-C4 bond. The N2 chemical shift in the 4-ethylpyrazole complex, 119.0 ppm, is 1.2 ppm upfield from that of the pyrazole complex. This is a small change, but it is in the direction of greater zinc complexation.

Another way to look at this is to compare the differences between average nitrogen shifts in the enzyme complexes to the difference between the averaged nitrogen shift in the free inhibitors. When this is done, the effect of substitution at the 4-position is expected to cancel and shifts may be analyzed for other effects. The average of

these nitrogen shifts in the 4-ethylpyrazole enzyme complex, 132.5 ppm, is 2.55 ppm upfield from the average in the pyrazole enzyme complex, while the chemical shift of free 4-ethylpyrazole is only 1.6 ppm upfield from that of free pyrazole. This result is consistent with somewhat greater zinc complexation in the 4-ethylpyrazole enzyme complex. This could be because of a small decrease in the N2-zinc bond distance and/or a small shift in an inner sphere-outer sphere equilibrium toward greater inner-sphere coordination.

#### IV. $^{15}\text{N}$ NMR Linewidths

##### LADH-NAD<sup>+</sup>-Pyrazole Complex

The observed linewidths for the nitrogen resonances of the LADH-NAD<sup>+</sup>-pyrazole complex are surprisingly narrow for a complex presumably of MW over 80,000. The linewidths collected in Table 8 include those of the pyrazole nitrogen doublets. The non-equivalent pyrazole nitrogens in the complex are coupled with an observed  $^1J_{\text{NN}}$  of  $10 \pm 2$  Hz, which means the actual observed linewidths of the individual resonances are 10 Hz less than those of the incompletely resolved doublets. The resonances do not arise from low-molecular-weight materials present in solution because the

Table 8.  $^{15}\text{N}$  Linewidths<sup>a</sup> of the Enzyme Ternary Complexes

Complex	Frequency <sup>b</sup> (MHz)	Linewidth (Hz)				NADR
		Pyrazole N2		Pyrazole N1		
		doublet	actual <sup>c</sup>	doublet	actual <sup>c</sup>	
LADH-NAD <sup>+</sup> -Pyrazole	18.25	20 <sup>±</sup> 2	~10	16 <sup>±</sup> 2	~6	
	50.68	30 <sup>±</sup> 2 <sup>d</sup>	~20	25 <sup>±</sup> 2 <sup>d</sup>	~15	5 <sup>±</sup> 4
LADH-NAD <sup>+</sup> -4-ethylpyrazole	50.68	40 <sup>±</sup> 7 <sup>d</sup>	e	20 <sup>±</sup> 7 <sup>d</sup>	e	

a Observed line width at half-height.

b Spectrometer operating frequency.

c (linewidth of doublet) - ( $^1J_{\text{NN}}$  of 10 Hz)

d One-bond  $^{15}\text{N}$ - $^{15}\text{N}$  coupling unresolved.

e  $^1J_{\text{NN}}$  not determined.

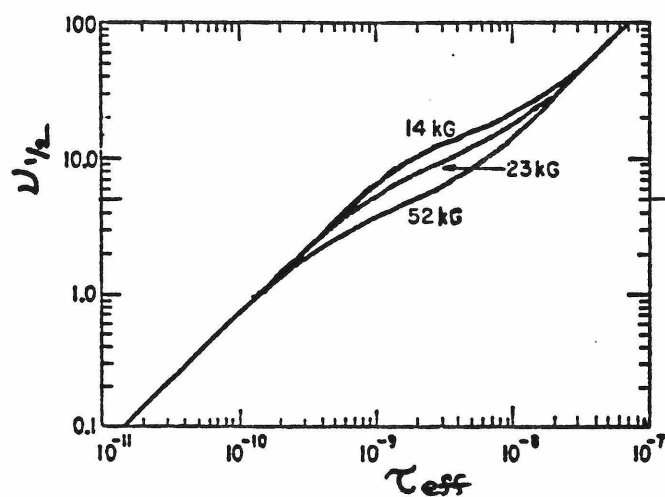


Figure 14. Plot of Linewidth,  $\nu_{1/2}$ , versus Effective Correlation Time,  $\tau_{eff}$ , Assuming Dipolar Relaxation (from reference 77).



complex from which they arise is not dialyzed.

For high-molecular-weight substances, a narrow linewidth necessarily implies a high degree of mobility of the nucleus from which the resonance arises.<sup>76</sup> Clearly, the effective correlation times for the pyrazole and nicotinamide portions of the inhibitor complex are much shorter than that expected for the bulk of the enzyme, despite the apparent tightness of bonding of the inhibitor to the coenzyme and catalytic zinc.

McGrath<sup>77</sup> has estimated the rotational correlation time for LADH to be  $4.6 \times 10^{-8}$  sec, using the Stokes-Einstein equation for an ellipsoid molecule of MW 80,000. A rough estimate of the correlation time may be obtained from the transverse relaxation time,  $T_2$ .  $T_2$  may be calculated from the natural linewidth at half-height,  $\nu_{1/2}$ , from the relation

$$T_2 = \frac{1}{\pi \nu_{1/2}} \quad .$$

When  $T_2$  is calculated using the observed linewidth, a lower limit to the actual transverse relaxation time is obtained because contributions to the linewidth from magnet inhomogeneity, residual spin-spin coupling or chemical

exchange possibly present have been ignored.<sup>31</sup> The values of  $T_2$  calculated in this manner for pyrazole N1 and N2 of LADH-NAD<sup>+</sup>-pyrazole at 18.25 MHz (  $\nu_H$  = 6 and 10 Hz, respectively) are 0.053 and 0.032 sec, respectively.

If it is assumed at this magnetic field that the relaxation mechanism is mainly dipolar, and the effective correlation time is less than about  $10^{-8}$  sec<sup>-1</sup>, then  $T_2$  is equal to the dipolar longitudinal relaxation time  $T_1$ , and the effective correlation time,  $\tau_{\text{eff}}$ , may be calculated from the equation<sup>31</sup>

$$\tau_{\text{eff}} = \frac{1}{T_1 (4.1 \times 10^9)} \quad .$$

The assumption of domination of the dipolar relaxation mechanism may not be an especially good one, because of the possibility of chemical-shift anisotropy (CSA) relaxation. However, as discussed later, CSA is estimated to make contributions of no more than about 30% and 25% to  $T_2$  of N1 and N2. For N1 and N2 at 18.25 MHz, the effective correlation times estimated in this way are  $4.6 \times 10^{-9}$  and  $7.6 \times 10^{-9}$  sec, respectively. These numbers are similar to those estimated from a plot of linewidth versus effective correlation time for situations where dipolar relaxation dominates, illustrated in Figure 14 and taken from reference

77. From this plot, the effective correlation times of N1 and N2 at 42 kGauss (18.25 MHz) are estimated to be  $2 \times 10^{-9}$  and  $5 \times 10^{-9}$  sec, respectively.

The effective correlation time for N1 is thus roughly estimated to be an order of magnitude shorter than that of the enzyme considered as a whole. Gust, Moon and Roberts<sup>33</sup> determined an effective correlation time of  $3.5 \times 10^{-9}$  sec for the guanidino  $\text{NH}_2^+$  groups based on  $^{15}\text{N}$   $T_1$  and NOE measurements, for lysozyme (MW 14,300), which has an estimated effective correlation as a whole of  $5 \times 10^{-9}$  sec. This difference is comparable to the difference between the correlation times of pyrazole N1 and LADH considered as a whole, indicating a degree of internal mobility of N1 similar to the guanidino  $\text{NH}_2^+$  groups.

The narrow lines observed for the pyrazole and nicotinamide nitrogens of the LADH- $\text{NAD}^+$ -pyrazole complex thus indicate that the structure of the complex is unlikely to be very rigid and it is possible that there is fast exchange between inner-sphere and outer-sphere coordination states of N2 of pyrazole to the active-site zinc. It is also possible that the resonances are narrow because of an unexpected flexibility of the pyrazole and nicotinamide moieties while maintaining direct coordination of N2 to the zinc. In the crystalline complex, there appears to be

sufficient room in the substrate-binding pocket for the pyrazole nucleus to rotate  $\pm 20^\circ$  around the N2-zinc axis,<sup>9</sup> but it is not clear whether this is enough to give the sharp  $^{15}\text{N}$  lines.

The mobility of the nicotinamide nitrogen may be explained in part by the fact that the nicotinamide moiety of binary LADH-coenzyme complexes is not very tightly bound, as evidenced by the observation that ADPR binds almost as strongly as NADH and more strongly than  $\text{NAD}^+$ .<sup>2</sup> The observation of this sharp  $^{15}\text{N}$  resonance suggests that  $^{15}\text{N}$  NMR of other enzyme-[N1- $^{15}\text{N}$ ]- $\text{NAD}^+$  complexes may prove fruitful.

#### LADH- $\text{NAD}^+$ -4-Ethylpyrazole Complex

The linewidths of the LADH- $\text{NAD}^+$ -4-ethylpyrazole complex indicate less mobility of the pyrazole nucleus in the 4-ethylpyrazole complex than in the LADH- $\text{NAD}^+$ -pyrazole complex (Table 8). The linewidth at 50.68 MHz was 40 Hz, one-third greater than that found in the pyrazole complex, while the N1 linewidth was about the same in both complexes. This can be explained if the 4-ethylpyrazole-enzyme residue interactions restrict mobility of N2 but not N1, and/or if the N2-zinc interaction is stronger than in the pyrazole complex, slightly immobilizing N2. This latter case would

contribute to the overall greater stability of the inhibitor complex and would explain the upfield shift of N2 relative to the pyrazole complex.

### Field Effects

In  $^{15}\text{N}$  NMR, in the absence of paramagnetic species and nuclear quadrupoles, the major mechanism of relaxation is often dipolar, but relaxation due to chemical-shift anisotropy (CSA) can be important, especially for  $\text{sp}$ - and  $\text{sp}^2$ -hybridized nitrogens.<sup>31</sup> If the relaxation of the observed nucleus is purely dipolar, then the linewidth of the resonance is predicted to decrease with increasing magnetic field, eventually becoming field-independent in the high-field limit.<sup>37</sup> However, when CSA contributes to the relaxation mechanism, the linewidth is field-dependent, the anisotropic contribution to  $T_2$  being inversely proportional to the square of the field, and the associated linewidth increasing quadratically as the field is increased.<sup>37</sup> The linewidths of N1 and N2 of the LADH- $\text{NAD}^+$ -pyrazole complex are observed to increase as the spectrometer frequency is increased from 18.25 to 50.68 MHz. The increase in field is 2.78-fold and the square of this increase is 7.7. The N1 and N2 linewidths only increase 2.5-fold and 2-fold, respectively, indicating at the most a one-third and one-

fourth contribution of CSA to the spin-spin relaxation. The observed increase in linewidth can reasonably be attributed to chemical-shift anisotropy broadening, but could also be caused by chemical-exchange broadening, which is also field-dependent. The occurrence of an equilibrium involving inner sphere-outer sphere zinc complexation of pyrazole could therefore contribute to the line-broadening at a higher field.

The sharp lines observed for the enzyme complex at 18.25 MHz indicate that if chemical exchange is occurring, it is fast on the NMR time scale, and the rate,  $k$ , is much greater than 2 times the separation in Hertz of the two exchanging resonances, that is,

$$k > 2\pi\Delta\nu \quad \text{or} \quad k > 2\pi(\Delta\delta \times 18.25 \text{ MHz})$$

where the separation in Hertz equals the chemical-shift difference in ppm ( $\Delta\delta$ ) times the field in Hertz. For exchange between fully hydrogen-bonded and zinc-complexed pyrazole, there should be a shift difference of about 33 ppm, which means an exchange rate greater than  $3.8 \times 10^3 \text{ sec}^{-1}$ . The line broadening at 50.68 MHz would be consistent with an intermediate exchange rate, that is, approaching

$$k \sim 2\pi(\Delta\delta \times 50.68 \text{ MHz}) \sim 1.1 \times 10^4 \text{ sec}^{-1}.$$

Because this rate is being approached from the fast exchange limit, it is a lower limit to the exchange rate. This

calculation of the possible rate of exchange between inner sphere- and outer sphere-coordination of pyrazole by the active-site zinc is of course only valid if the line broadening at high field is in fact caused by chemical exchange and not CSA.

#### V. Relevance to Mechanism of LADH

The structure of the LADH-NAD<sup>+</sup>-pyrazole complex may provide insight into the role of the zinc ion in binding and activation of substrate. Our <sup>15</sup>N results indicate that, in solution, the active site of the enzyme promotes the formation of an entity where pyrazole is substantially directly coordinated to the active-site zinc and also covalently bound to the nicotinamide moiety. The structure of the LADH-NAD<sup>+</sup>-pyrazole complex (Figure 15 ) is very similar to the proposed structure<sup>1,2</sup> of the transition state of the LADH reaction where substrate is inner-sphere coordinated to zinc (Figure 16). The zinc may thus help to orient the substrate within the substrate-binding pocket correctly in relation to the nicotinamide moiety for stereospecific hydride transfer to occur, while at the same time acting as a Lewis-acid catalyst in the reaction.

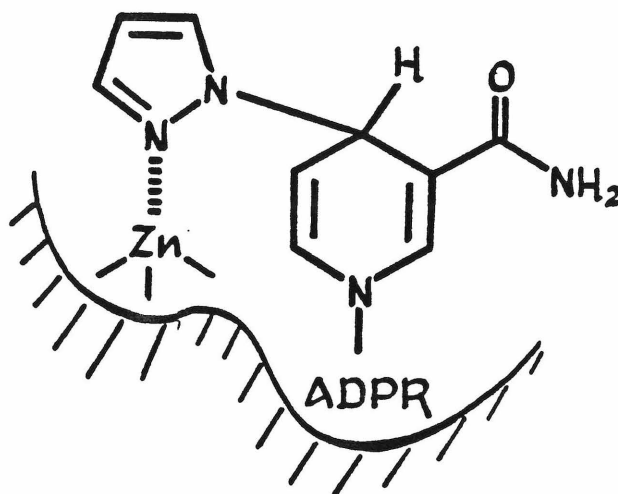


Figure 15. Proposed Structure of LADH-NAD<sup>+</sup>-Pyrazole, Based on <sup>15</sup>N NMR Results, Indicating Substantial (60-100%) Direct Zinc Complexation.

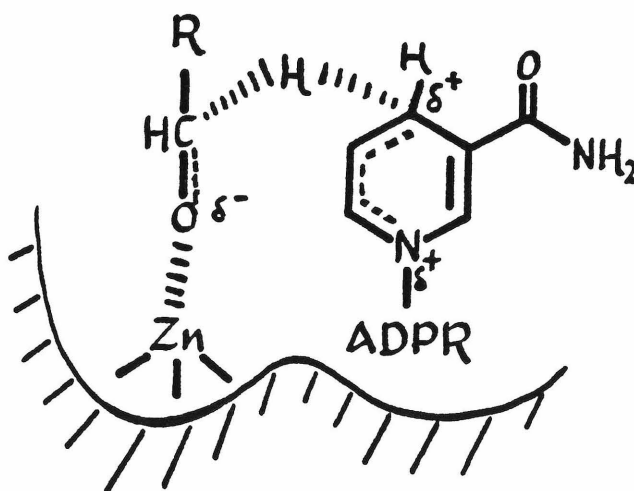


Figure 16. Proposed Structure of the Transition State of the LADH Oxidation of Alcohol.



Direct zinc-coordination of alcohol substrate would decrease its  $pK_a$ , possibly to a point where substrate binds as the alcoholate as previously proposed,<sup>1,2</sup> thus facilitating transfer of hydride from substrate to  $NAD^+$ . In the reverse reaction, polarization of the carbonyl group of aldehyde substrate by the active-site zinc would create partial positive charge on C1, facilitating hydride transfer from NADH to substrate. X-ray crystallographic studies<sup>7-9</sup> have supported this mechanism by indicating direct coordination of substrate or inhibitor to zinc. However, because the crystal structures may differ from the solution structures, it is significant that our results demonstrate a structure of LADH- $NAD^+$ -pyrazole in solution which is similar to the crystal structure.

## CONCLUSIONS

We have found that in solution, the LADH-NAD<sup>+</sup>-pyrazole complex has chemical shifts for the pyrazole N1 and nicotinamide ring nitrogens which suggest bond formation between pyrazole N1 and nicotinamide C4, in agreement with the model first proposed by Theorell and Yonetani.<sup>24</sup> The chemical shift of the pyrazole N2 for the ternary complex is indicative of substantial (60-100%) inner-sphere coordination to the active-site zinc. While these results do not exclude partial outer-sphere coordination, they do demonstrate that the solution structure of the ternary complex (Figure 15) is very similar to that found for the crystalline enzyme complex.

The LADH-NAD<sup>+</sup>-4-ethylpyrazole complex was found to be very similar in structure to the LADH-NAD<sup>+</sup>-pyrazole complex, with possibly slightly stronger coordination of N2 to the active-site zinc.

This is the largest enzyme complex (MW over 80,000) for which <sup>15</sup>N spectra have been reported. The narrow <sup>15</sup>N resonances observed for the LADH-NAD<sup>+</sup>-pyrazole complex are noteworthy for such a high-molecular-weight complex. It would appear that the application of NMR to the general investigation of small molecules bound to large biomolecules should not be prejudged to give such broad lines as to be worthless to attempt.

## References:

1. Branden, C.-I., Jornvall, H., Eklund, H., and Furugren, B. (1975) Enzymes, 3rd Ed. 11, 103.
2. Klinman, J. P. (1981) Crit. Rev. Biochem. 10, 39.
3. Jornvall, H. (1970) Eur. J. Biochem. 16, 25.
4. Jornvall, H., and Pietruszko, R. (1972) Eur. J. Biochem. 25, 283.
5. Jornvall, H. (1977) Eur. J. Biochem. 72, 443.
6. Eklund, H., Nordstrom, B., Zeppezauer, E., Soderlund, G., Ohlsson, I., Boiwe, T., Soderberg, B.-O., Tapia, O., Branden, C.-I., and Akeson, A. (1976) J. Mol. Biol. 102, 27.
7. Eklund, H., Plapp, B. V., Samama, J.-P., Branden, C.-I. (1982) J. Biol. Chem. 257, 14349.
8. Eklund, H., Samama, J.-P., Wallen, L., Branden, C.-I., Akeson, A., and Jones, T. A. (1981) J. Mol. Biol. 146, 561.
9. Eklund, H., Samama, J.-P., and Wallen, L. (1982) Biochemistry 21, 4858.
10. Plapp, B. V., Eklund, H., and Branden, C.-I. (1978) J. Mol. Biol. 122, 23.
11. Cedergren-Zeppezauer, E., Samama, J.-P., and Eklund, H. (1982) Biochemistry 21, 4895.
12. Branden, C.-I. (1977) in "Alcohol and Aldehyde Metabolizing

- Systems" (Thurman, R. G., Williamson, J. R., Drott, H. R., and Chance, B., Eds.) Vol.II, Academic Press, New York.
13. Samana, J. P. Zepperzauer, E., Biellman, J. F., and Branden, C.-I. (1977) Eur. J. Biochem. 81, 403.
  14. Wratten, L. C., and Cleland, W. W. (1963) Biochemistry 2, 935.
  15. Shore, J. O., Gutfreund, H., Brocks, R.L., Santiago, D., and Santiago, P. (1974) Biochemistry 13, 4185.
  16. Prince, R. H. and Woolley, P. R. (1973) Bioorg. Chem. 2, 337.
  17. Woolley, P. (1975) Nature (London) 258, 677.
  18. Boiwe, T., and Branden, C.-I. (1977) Eur. J. Biochem. 77, 173.
  19. Sloan, D. L., and Young (1974) Fed. Proc., Fed. Am. Soc. Exp. Biol. 33, 1244.
  20. Sloan, D. L., Young, J. M., and Mildvan, A. S. (1975) Biochemistry 14, 1998.
  21. Sloan, D. L., Jr., Young, J. M., and Mildvan, A. S. (1975) in "Structure and Conformation of Nucleic Acids and Protein-Nucleic Acid Interactions (Surdavalingam, M. and Rao, S. T., Eds.) University Park Press, Baltimore.
  22. Drysdale, B.-E., and Hollis, D. P. (1980) Arch.

Biochem. Biophys. 205, 267.

23. Deis, F. H., and Lester, D. (1979) in "Biochemical Pharmacology of Ethanol" (Majchrowicz, E., and Noble, E. P., Eds.) Vol 2, p. 303, Plenum Press, New York.
24. Theorell, H., and Yonetani, T. (1963) Biochem. Z. 338, 537.
25. Theorell, H., Yonetani, T., and Sjoberg, B. (1969) Acta Chem. Scand. 23, 255.
26. Shore, J. D., and Gilleland, M. J. (1970) J. Biol. Chem. 245, 3422.
27. Dahlbom, R., Tolf, B. R., Akeson, A., Lundquist, G., and Theorell, H. (1974) Biochem. Biophys. Res. Commun. 57, 549.
28. a) Van Eys, J. (1958) J. Biol. Chem. 237, 1203.
28. b) Van Eys, J. Stolzenbach, F. E., Sherwood, L., and Kaplan, N. O. (1958) Biochim. Biophys. Acta 27, 63.
29. Angelis, C. T. (1980) Doctoral Thesis, University of California, Riverside.
30. Bobsein, R. B., and Myers, R. J. (1980) J. Am. Chem. Soc. 102, 2454.
31. Levy, G. C., and Lichter, R. L. (1979) "Nitrogen-15 Nuclear Magnetic Resonance Spectroscopy," Wiley and Sons, New York.
32. Kanamori, K., and Roberts, J. D., (1983) Accts. Chem.

Res, In Press.

33. Gust, D., Moon, R. B., and Roberts, J. D., (1975) Proc. Natl. Acad. Sci., USA 72, 4696.
34. Bachovchin, W. W., and Roberts, J. D. (1978) J. Am. Chem. Soc. 100, 8041.
35. Wehrli, F. W., and Wirthlin, T. (1976) "Interpretation of Carbon -13 NMR Spectra" p. 138, Heyden, New York.
36. Wuthrich, K. (1976) "NMR in Biological Research: Peptides and Proteins", p. 147, American Elsevier, New York.
37. Bothner-By, A. A., and Dadok, J. (1979) in "NMR and Biochemistry" (Opella, S. J., and Lu, P., Eds.) pp. 169-202, Marcel Dekker, New York.
38. Czeisler, J. L., and Hollis, D. P. (1973) Biochemistry 12, 1683.
39. Hollis, D. P. (1967) Biochemistry 6, 2080.
40. Anderson, D. C., and Dahlquist, F. W. (1982) Biochemistry 21, 3578.
41. Bernhard, S. A., Dunn, M. F., Luisi, P.-L. and Schack, P. (1970) Biochemistry 9, 185.
42. Anderson, D. C., Dahlquist, F. W. (1982) Biochemistry 21, 3569.
43. Young, J. M., and Mildvan, A. S., (1977) in "Alcohol and Aldehyde Metabolizing Systems" (Thurman, R. G.,

Williamson, J. R., Drott, H. R., and Chance, B., Eds.)  
Vol. II, Academic Press, New York.

44. Andersson, I., Maret, W., Zeppezauer, M. Brown, R. D.,  
III, and Koenig, S. H. (1981) Biochemistry 20, 3424.
45. Bobsein, R. B., and Myers, R. J. (1981) J. Biol. Chem.  
256, 5313.
46. Dunn, M. F., Dietrich, H., MacGibbon, A. K. H.,  
Koerber, S. C., and Zepperauer, M. (1982) Biochemistry  
21, 354.
47. Jones, R. G. (1949) J. Am. Chem. Soc. 71, 3994.
48. Klimko, V. T., and Skoldinov, A. P. (1959) Zh. Obsch.  
Khim. 29, 4027-4029; (1959) J. Gen. Chem. USSR 29,  
3987.
49. Breitmaier, E., and Gassenman, S. (1971) Chem. Ber.  
104, 665.
50. Oppenheimer, N. J., and Davidson, R. M. (1980) Org.  
Magn. Reson. 13, 14.
51. Karrer, P., and Stare, F. J. (1937) Helv. Chim. Acta  
20, 418.
52. Hawkes, G. F., Randall, E. W., Elguero, J., and Marzin,  
C. (1977) J. Chem. Soc. Perkin Trans. 2, 1024.
53. Bulusu, S., Autera, J. R., and Axenrod, T. (1974)  
in "Nuclear Magnetic Resonance Spectroscopy of Nuclei  
Other than Protons" (Axenrod, T. and Webb., G. A.,

Eds.) Wiley, New York.

54. Schuster, I. I., Dyllick-Brenzinger, C., and Roberts, J. D. (1979) J. Org. Chem. **44**, 1765.
55. Dittmer, D. C. and Kolyer, J. M. (1963) J. Org. Chem. **28**, 2288.
56. Oppenheimer, N. J., Arnold, L. J., Jr., and Kaplan, N. O. (1978) Biochemistry **17**, 2613.
57. Karle, I. L. (1961) Acta Crystallogr. **14**, 497.
58. Cook, P. F., Oppenheimer, N. J., and Cleland, W. W. (1981) Biochemistry **20**, 1817.
59. Branden, C.-I., and Eklund, H. (1978) Mol. Interact. Proteins, Ciba Found. Symp., 63.
60. Eklund, H., and Branden, C.-I. (1979) J. Biol. Chem. **254**, 3458.
61. Kost, A. N., and Grandberg, I. I. (1966) Adv. Heterocycl. Chem. **6**, 347.
62. Jagil, G. (1967) Tetrahedron **23**, 2855.
63. Kanamori, K., unpublished results.
64. a) Minato, H., Yamazaki, E., and Kobayashi, M. (1976) Chem. Lett., 525.  
b) Ohnishi, Y., Minato, H., Okuma, K., and Kobayashi, M. (1977) Chem. Lett., 525.
65. Alei, M., Jr., Morgan, L. O., and Wageman, W. E. (1978) Inorg. Chem. **17**, 2288.



66. Alei, M., Jr., Morgan, L. O., and Wageman, W. E.  
(1981) Inorg. Chem. 20, 940.
67. Buchanan, G. W., and Stothers, J. B. (1982) Can. J. Chem. 60, 787.
68. Happes, J. A., and Morales, M. (1966) J. Am. Chem. Soc. 88, 2077.
69. Nee, M., and Roberts, J. D. (1982) Biochemistry 21, 4920.
70. a) Ahrland, S., and Bjork, N.-O. (1975) Coord. Chem. Rev. 16, 115.  
b) Daugherty, N. A., and Swisher, J. H. (1968) Inorg. Chem. 7, 1651.  
c) Reedijk, J. (1970) Recl. Trav. Chim. Pays-Bas 89, 993.
71. Heslop, R. B., and Jones, K. (1976) "Inorganic Chemistry" pp. 580-590, Elsevier Scientific, New York.
72. Barvinok, M. S., and Lukina, L. G. (1977) Zh. Neorg. Khim. 22, 2167.
73. Terheijden, J., Driessen, W. L., and Groeneveld, W. L. (1980) Transition Met. Chem. 5, 346.
74. Hughes, M., and Prince, R. H. (1978) J. Inorg. Nucl. Chem. 40, 703.
75. Blumenstein, M., and Raftery, M. A. (1973) Biochemistry 12, 3585.

76. Jardetzky, O. (1979) in "NMR and Biochemistry"  
(Opella, S. J., and Lu., P., Eds.) pp. 141-167,  
Marcel Dekker, New York.